Deltares

Enabling Delta Life

Variability of the cone penetration resistance

Deltares

Variability of the cone penetration resistance

De heer ing. T.A. van Duinen

Deltares

Title
Variability of the cone penetration resistance

Client	Project	Attribute	Pages
Rijkswaterstaat Water, Verkeer en Leefomgeving, UTRECHT	11202225-005	11202225-005-GEO-0013	58

Keywords
Spatial variability, cone penetration resistance, correlation length, variance reduction factor

Summary
In the WBI 2017 guideline (I&M, 2016) for slope stability the Appendices G, H and I describe the application of CPT's and the approach to use CPT data to determine parameters for slope stability analyses. The variability of the shear strength within a dike section based on a number of CPT's has been showed to be considerable. Within the WBI guidelines it is not specified yet how to deal with this variability of the soil properties in the assessment of a dike section. A site investigation is performed to investigate the variability of the cone penetration resistance. Literature research is performed in order to apply recent knowledge about interpretation and modelling spatial variability of soil properties. Based on this research it can be concluded that the characteristic lower bound of the cone penetration resistance for a dike section has to be derived from a series of CPT's. This series of CPT's represent the variability of the soil much more than one CPT. These series of CPT's can belong to a dike section or a WBI-SOS segment for example. Averaging of variability along a slip surface can be taken into account by the variance reduction factor as described by TAW (2002). This variance reduction factor seems to be also very variable with dense datasets.

References
KPP-programma 2018 – WK01 – WBI 2023

Version	Date	Author	Initials	Review	Initials	Approval	Initials
1.0	jan. 2019	ing. T.A. van Duinen		dr.ir. W. Kanning		ir. L. Voogt	

Status
final

Contents

1 Introduction

1.1 Background

For assessments and design of slope stability of flood defences cone penetration tests (CPT's) are important tests for soil investigation. Both for soil layering and shear strength parameter determination. In the WBI 2017 guideline (I&M, 2016) for slope stability the Appendices G, H and I describe the application of CPT's and the approach to use CPT data to determine parameters for slope stability analyses.

CPT's can be performed to determine the in situ undrained shear strength and stress history (state) of soft soils. This is because of the idea that the spatial variability of the undrained shear strength and stress history is such large, that a high density of local measurements (horizontal and vertical) is needed to avoid prohibitively conservative choices. Executing bore holes with large distances between the bore holes and laboratory tests on samples from these bore holes is thought to be insufficient for an accurate and reliable insight in the spatial variability of the parameters.

In the 'Dijken op Veen' ('Dikes on peat') project (Deltares, 2014) an approach is developed where CPT's should be carried out in each cross section where a slope stability analysis has to be performed. About the required interval between these cross sections or CPT's within the dike section no instruction is given. Using the CPT data to calculate a characteristic lower bound value of the undrained shear strength this characteristic lower bound value is about 35% lower than the mean value of the undrained shear strength. This is likely due to the effect of the uncertainty due to spatial variability and the effect of the transformation uncertainty. The transformation uncertainty accounts for the uncertainty due to the transformation from cone penetration resistance to undrained shear strength based on an empirical correlation between laboratory measurements of the undrained shear strength and cone penetration resistance. This transformation uncertainty causes the majority of the gap between mean value and characteristic lower bound. Transformation uncertainty is estimated to be about two times the uncertainty due to heterogeneity (Deltares, 2014).

Within the WBI-project this approach is also adopted. However, within the WBI system one works with dike sections, which are defined as stretches of a dike with more or less homogeneous geometry, hydraulic boundary conditions, subsoil etc. In such a dike section several CPT's can be available. The variability of the shear strength within a dike section based on a number of CPT's has been showed to be considerable. Within the WBI guidelines it is not specified yet how to deal with this variability of the soil properties in the assessment of a dike section. Within the WBI system it is the aim to determine a realistic probability of failure for a dike section. So it is not intended to determine the probability of failure based on worst case estimations and combinations of worst case estimations, but to find design values or distributions of shear strength parameters that reflect the dike behaviour well.

1.2 Research question

When a series of CPT's with regular distances between the CPT's are performed and analysed a local low value of the undrained shear strength can occur. In that case several scenarios about the spatial variability of the shear strength are possible:

- The low value of the undrained shear strength in a local CPT might show a local soft soil layer with dimensions large enough to affect the stability, for example a small channel of meters or tens of meters width and filled with soft material. This small channel might potentially induce a slope failure.
- The low value of the undrained shear strength in a local CPT might be a very local soft part of a soil layer with a limited impact on the shear strength. In this case the shear strength on a slip surface of a potential slope instability averages on the scale of the slip surface.

From these scenarios and the problem definition as described in the background the question arises how to deal with the variability of the cone penetration resistance as found with CPT's in a dike section and which value of the cone penetration resistance or undrained shear strength should be applied in a slope stability analysis?

1.3 Aim of the project

The aim of the project is to compose an instruction for the schematization of the spatial variability of soil layers based on one or more CPT's for the purpose of the assessment of the slope stability of flood defences. The instruction will be fitted onto the WBI system where the assessment is performed for dike sections as mentioned before. Starting point is the natural variability of the subsoil, i.e. variability induced by differences in the sedimentary environment, variability of soil properties, effects of creep, ripening and variability in pore water pressures etc. The effect of averaging of the spatial variability will be taken into account. The effect of a coincidental pre-loading of the soil in a dike section in the past due to human activities is outside the scope of this research. The transformation is outside the scope of this report.

1.4 Approach

To analyse the natural heterogeneity of the cone penetration resistance three series of CPT's are performed along the drainage canal "Achterwaterschap" in the western part of the Alblasserwaard. These series of CPT's are performed at three locations. At each location 15 CPT's with measurement of cone resistance are performed within a row of 100 m length. So the distance between the CPT's is 7.0 m. Five additional CPT's with measurement of cone resistance, sleeve friction and pore water pressure are performed at each location to be used for the interpretation of the stratigraphy of the subsoil. Because of this set-up a relatively large part of the heterogeneity of the subsoil on the scale of a potential slope failure can be investigated. At the three sites various soil layers from different sedimentary environments are available. Therefore different patterns of spatial variability can be expected at these sites. The CPT data is analysed to determine the stratigraphy of the subsoil and the statistics of the measured cone penetration resistance. A literature research is performed first in order to apply recent knowledge about interpretation and modelling spatial variability of soil properties.

This research started in 2017. In 2017 cone penetration tests from regular site investigations by the waterboards were analysed. In these site investigations the distances between the cone penetration tests were 100 m or more as commonly applied. The concerning dike sections are Waaldijk Tiel – Waardenburg (Waterboard Rivierenland, WSRL) with 71 class 1 CPT's in the crest and at the for- and hinterland, Balgzanddijk en Amsteldiepdijk (Waterboard Hollands Noorderkwartier) with 30 class 2 CPT's in the crest and at the inner berm, Achterwaterschap in the Alblasserwaard (Waterboard Rivierenland) with 72 class 1 CPT's at the crest. The results of this research in 2017 are used in the additional research as described in this report.

1.5 Outline

Chapter 2 describes the set-up of the research along the “Achterwaterschap”, which consisted in a site investigation and analyses. A literature review is performed about the theory behind interpretation and modelling of spatial variability. This can be found in Chapter 3. Chapter 4 gives a recapitulation of the most important findings in the research of 2017 on the same topic. In Chapter 5 the interpretation and analysis of the data from the site investigation at three locations along the “Achterwaterschap” is described. The results of the 2017 research and the results of the analyses of the data from the “Achterwaterschap” are discussed in Chapter 6. The conclusions and recommendations can be found in Chapter 7 and 8 respectively. The consequences for the WBI 2017 instrumentarium are summarized in Chapter 9 (in Dutch).

2 Set-up of the research

2.1 Site investigation

The site investigation at the three locations along the drainage canal “Achterwaterschap” in the western part of the Alblasserwaard consists of one row of 100 m length in which 15 cone penetration tests with class 1+ cones, the so called “dyke cone”, are performed. So the distance between these cone penetration tests is 7.0 m. Furthermore 5 cone penetration tests with class 1 cones are performed, which are located closely to the class 1+ cones. The class 1 cones measure cone resistance, sleeve friction and pore water pressure. The class 1+ cones only measure cone resistance, but they measure cone resistance with a measurement accuracy of 7.5 kPa, whereas the measurement accuracy of the class 1 cone resistance is 35 kPa. The high measurement accuracy of the class 1+ cone is very important to measure the cone resistance in the soft soils in the Alblasserwaard very accurately. Especially because this location typically has very low effective stresses. Figure 2.1, Figure 2.2 and Figure 2.3 show the locations of the site investigations with the performed in situ tests.

Figure 2.1 Situation of the site AC 075 at the north dike of the drainage canal Achterwaterschap with the locations of the class 1+ cones (red points) and class 1 cones (blue points).

Figure 2.2 Situation of the site AC 090 at the north dike of the drainage canal Achterwaterschap with the locations of the class 1+ cones (red points) and class 1 cones (blue points).

Figure 2.3 Situation of the site AC 251 at the south dike of the drainage canal Achterwaterschap with the locations of the class 1+ cones (red points) and class 1 cones (blue points).

2.2 Analysis

The results from the 5 class 1 cones at each location are used in a first step to characterize the stratigraphy of the subsoil. This is because these cones measure cone penetration resistance, sleeve friction and pore water pressure. So, these cones give more information than the class 1+ cones. After that the cone penetration resistances from the 15 class 1+ cones at each location are used to characterize the stratigraphy of the subsoil between the locations of the class 1 cones. Information from bore holes as performed by Waterboard Rivierenland is also used for the characterization of the subsoil.

The CPT data is interpreted using the Begemann (1965) classification system and the Been and Jefferies (1992) classification system. In Dutch engineering practise the classification of Begemann (1965) is a very common method. Begemann defined values of the friction ratio and related soil types to these friction ratio values. The friction ratio R_f is the ratio of the sleeve friction resistance f_s to the cone tip resistance q_c in percentages $\left(R_f = f_s/q_c \times 100\%\right)$.

Been and Jefferies (1992) modified the classification chart of Jefferies and Davies (1991) and uses the dimensionless parameter group $Q_t\left(1 - B_q\right) + 1$ versus the normalised friction ratio F_r. Q_t is the normalized dimensionless cone penetration resistance:

$$Q_t = \frac{(q_t - \sigma_{vi})}{\sigma'_{vi}} = q_{net}/\sigma'_{vi} \quad (2.1)$$

with net cone resistance:

$$q_{net} = q_t - \sigma_{vi} \quad (2.2)$$

and corrected cone resistance:

$$q_t = q_c + u_2(1 - a) \quad (2.3)$$

where:

q_t	corrected cone resistance for pore pressure effects (MPa).
σ_{vi}	in situ total vertical stress (MPa).
σ'_{vi}	in situ vertical effective stress (MPa).
q_{net}	net cone resistance corrected for pore pressure effects and in situ total vertical stress (MPa).
q_c	measured cone tip resistance (MPa).
u_2	pore water pressure measured just behind the cone during penetration (MPa).
a	area ratio (that area affected by the pore water pressure) (-).

The corrections for measured pore water pressure and total vertical stress are applied as given in equations (2.2) and (2.3). These corrections are based on the work of Campanella et al (1982), Robertson et al (1990), Robertson et al (1999), Zhang et al (2002) and others. The correction for pore water pressure has to be applied because of the pore water pressure effects acting in the joints of the penetrometer.

The normalised friction ratio is:

$$F_r = (f_s/q_{net}) \times 100\% \quad (2.4)$$

with:

F_r	normalized friction ratio (%).
f_s	sleeve friction resistance (MPa).

In the Been and Jefferies (1992) approach the drainage conditions around the cone during penetration are incorporated with the normalised excess pore water pressure B_q:

$B_q = (u_2 - u_0)/q_{net}$ (2.5)
with u_0 the stationary pore water pressure (MPa).

The boundaries between the soil types following the Been and Jefferies (1992) approach are marked with I_c:

$$I_c = \sqrt{\left(3 - log\left(Q_t\left(1 - B_q\right) + 1\right)\right)^2 + \left(1.5 + 1.3log\left(F_r\right)\right)^2} \quad (2.6)$$

The different soil types are given in Table 2.1.

Zone	I_c (-)	Soil classification
2	I_c > 3.22	Organic soils
3	2.76 < I_c < 3.22	Clays
4	2.40 < I_c < 2.76	Clayey silt to silty clay
5	1.80 < I_c < 2.40	Silty sand to sandy silt
6	1.25 < I_c < 1.80	Sands: clean to silty
7	I_c < 1.25	Gravelly sands

Table 2.1 Boundaries of the soil types according to Been and Jefferies (1992).

After the interpretation of the stratigraphy and the corrections of the CPT data statistical analyses on the CPT data are performed. Therefore the theory as discussed in the following chapter is applied.

3 Literature review

3.1 Dutch practice

In Dutch practice for assessment and design of flood defences the characteristic lower bound value of soil properties which are related to slope instability analyses, such as friction angle or undrained shear strength, is calculated according to TAW (2002) and Calle (2007) with:

$$X_{loc\ gem,char} = \hat{\mu}_X - t^{0.95}_{N_{tot-1}} \hat{\sigma}_{X,reg} \sqrt{\frac{1}{N_{tot}} + \Gamma^2} \quad (3.1)$$

where:

$X_{loc\ gem,char}$	characteristic lower bound value of parameter X.
$\hat{\mu}_X$	estimated mean value of parameter X.
$t^{0.95}_{N_{tot-1}}$	student t factor for 5% lower bound value (95% probability of exceedance) (-).
$\hat{\sigma}_{X,reg}$	standard deviation of parameter X of a regional dataset.
N_{tot}	number of observations (-).
Γ^2	variance reduction factor (-).

In equation (3.1) the term $\sqrt{\frac{1}{N_{tot}} + \Gamma^2}$ accounts for averaging of the spatial variability of the soil properties along a slip surface of a potential slope failure. The parameter Γ^2 is a dimensionless reduction factor that lies between 0 and 1. This parameter reduces the standard deviation the more the fluctuations of a parameter tend to cancel in the process of spatial averaging (Vanmarcke, 1977). According to Calle (2007 and 2008) the parameter Γ^2 can be determined from the variance ratio α between the local variance σ_{loc} and the regional variance σ_{reg} of a dataset, since the local variations tend to average out while the regional variations do not. This is because the local variations are mainly occurring vertically and tend to have much smaller correlation lengths than the size of the failure plain. The variance reduction factor is: $\Gamma^2 = 1 - a$ with $a = \sigma^2_{loc}/\sigma^2_{reg}$.

In TAW (2002), the default variance ratio α = 0.75 (Γ^2 = 0.25) for regional datasets. This value is based on analyses of regional data sets of shear strength parameters of different soil layers derived from Dutch cell tests. These analyses indicated a range of α between 0.5 and 1.0. A very accurate determination of α was not possible. So α is an uncertain parameter. The value of α is therefore a pragmatic choice. In TAW (2002) it is suggested that the vertical correlation length is some decimeters and the horizontal correlation length is about 50 to 100 m. The correlation length is the distance in which the correlation between soil properties decreases from 1 to 0. For local datasets where the dataset covers the scale of a potential slip surface the default variance ratio α = 1.0 (Γ^2 = 0) (TAW, 2002) and all uncertainty (except the statistical uncertainty due to limited number of samples) averages.

The approach of TAW (2002) and Calle (2007) is based on a model for spatial distribution of soil parameters with the assumption that the local values of a soil parameter vary in horizontal and vertical direction around a regional average (Calle, 2007 and 2008). Furthermore it is assumed that the local variation of a certain parameter is smaller than the regional variation of that parameter. The correlation between soil properties from samples coming from one bore hole is assumed to be much larger than the correlation between soil properties from samples coming from different bore holes at larger distances. The variability in vertical direction is thought to average nearly completely on the scale of a slope failure, as the vertical correlation length is only some decimeters. The variance reduction in horizontal direction however is thought to be limited (TAW, 2002).

Calle (2008) states that each site investigation should be performed in a way that it is possible to determine the ratio between the local variance and regional variance. To be able to calculate the local variance a number of 4 to 6 samples per soil layer and per bore hole will be required.

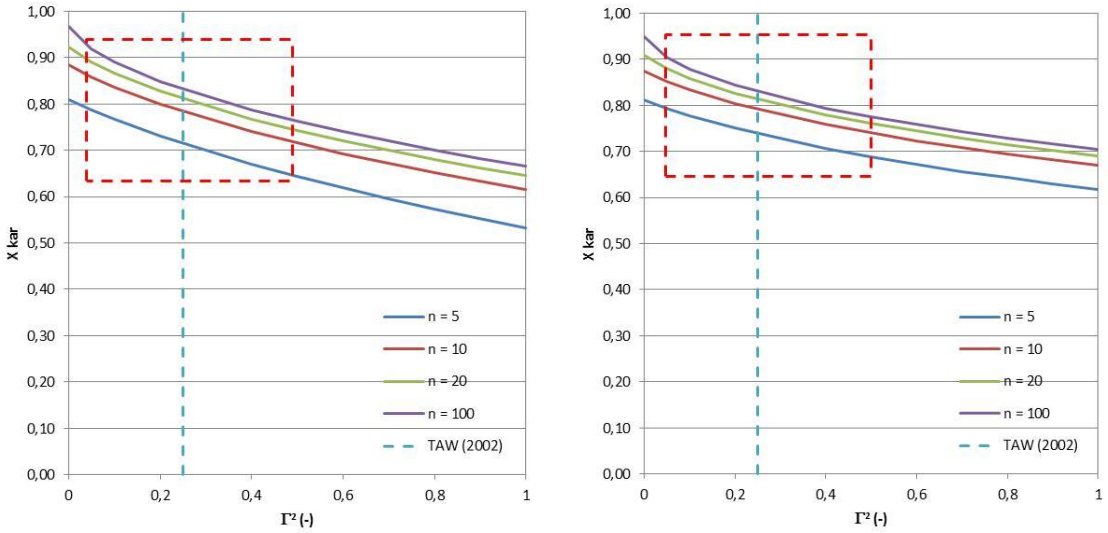

Figure 3.1 Relation between variance reduction factor, number of tests and characteristic lower bound value. Normal distribution (left) and log normal distribution (right) (CoV = 0.2).

The relevance of the reduction factor Γ^2 for the characteristic lower bound is illustrated in Figure 3.1 using equation (3.1). The mean value is 1.0 and the characteristic lower bound value is presented relative to the mean value. The dashed blue line shows the default value of the reduction factor Γ^2 for regional datasets according to TAW (2002). The dashed red box marks the range of the expected values of Γ^2. Depending on the number of observations and the value of the reduction factor the characteristic lower bound can be remarkable lower than the mean value. So, it might be an interesting option to optimize the reduction factor to get a more accurate characteristic lower bound value.

3.2 Literature

In geotechnical practice it is not very common to account for correlation between soil properties in horizontal direction (Cao et al, 2017). Usually the assumption is that a strong horizontal correlation results in a conservative design. Based on synthetic data, De Gast et al (2018) performed a probabilistic analysis and showed that the factor of safety of a slope of a dike may increase by about 10% when the horizontal and vertical spatial scale of fluctuation is taken into account. From this study De Gast et al (2018) suggest to perform site investigations where CPT's are located in groups. When using groups of CPT's the vertical and horizontal scale of fluctuation can be determined from the CPT data. This recommendation in essence is comparable with the recommendation of Calle (2008) who suggested to determine the reduction parameter Γ^2 from the ratio between the local variance and regional variance based on the results of site investigations.

According to Cao et al (2017) two categories of models to describe spatial variability of soil properties are available: finite scale model (short-memory) and fractal model (statistically self-similar or long-memory; Fenton, 1999).

3.2.1 Spatial variability based on finite scale models

Correlation function

Using the finite scale model the correlation length of a soil parameter can be determined by fitting the theoretical correlation function on the empirical correlation function. Various theoretical correlation functions can be used (Cao et al, 2017), however the exponential function according to Markov is used very often. Spry et al (1988) states that a physical base to prefer one of these theoretical correlation functions don't exist. The Markov model has an exponentially decaying correlation function (Fenton, 1999):

$$\rho(\tau) = exp\left(-\frac{2|\tau|}{\theta}\right) \quad (3.2)$$

where:

$\rho(\tau)$ correlation coefficient between two points separated by τ(-).
τ lag distance (m).
θ a distance called the 'scale of fluctuation' (m).

Following Fenton (1999) the 'scale of fluctuation' may be loosely interpreted as the separation distance beyond which soil properties are largely uncorrelated. This model is considered to be a finite-scale model because the correlation dies out very rapidly for separation distances $\tau > \theta$; the area under this function, in particular, is finite (Fenton, 1999).

The sample correlation $\hat{\rho}(\tau_j)$ is obtained by normalizing as given by Fenton (1999):

$$\hat{\rho}(\tau_j) = \frac{\hat{C}_{(\tau_j)}}{\hat{C}_{(0)}} \quad (3.3)$$

where:

$\hat{C}_{(\tau_j)}$ estimator of the covariance function at discrete lag τ_j.
$\hat{C}_{(0)}$ is the same as the estimated variance $\hat{\sigma}_X^2$.

The sample covariance function is obtained from the moment estimator (Fenton, 1999):

$$\hat{C}(\tau_j) = \frac{1}{n-j}\sum_{i=1}^{n-j}(x_i - \hat{\mu}_X)(x_{i+j} - \hat{\mu}_X) \text{ with } j = 0, 1, \ldots, n-1 \quad (3.4)$$

where:

x_i observed value of X_z.
$\hat{\mu}_X$ estimated mean of X_z.
n number of observations in sample of X_z.
j number of lag distances τ.

The data, $x_i, i = 1, 2, \ldots, n$, are to be collected at a sequence of equispaced points along a line. Based on the calculated sample correlation at various lags ($\hat{\rho}(\tau_j)$), an autocorrelation function can be fitted, see Figure 3.2.

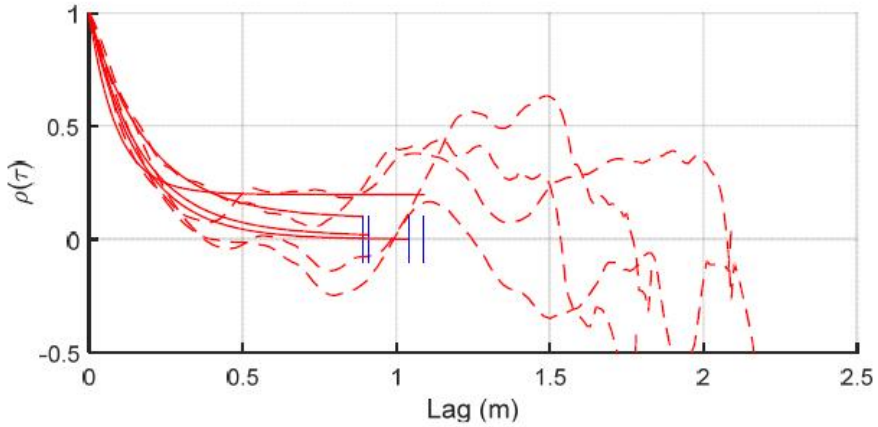

Figure 3.2 Example of empirical correlation function and fitted theoretical correlation function showing vertical correlation of CPT data from De Gast et al (2017).

In Figure 3.2 an example of an empirical correlation function and a fitted theoretical correlation function is given.
One of the major difficulties with the sample correlation function resides in the fact that it is heavily dependent on the estimated mean (Fenton, 1999). When the soil shows significant long-scale dependence, characterized by long-scale fluctuations, then the estimated mean value is almost always a poor estimate of the true mean value.
According to Fenton the estimator $\hat{\rho}(\tau)$ will typically dip below zero due to bias problems even when the field is actually highly positively correlated. However, the sample correlation function is a good estimator of short-scale processes as long as the correlation length is much shorter than the sampling domain. The sample correlation function fails to provide any useful information about large-scale processes. Furthermore, there needs to be sufficient data points with smaller lag distance than the correlation distance in order to compute the correlation distance. De Gast et al (2017) points out that, while constructing the experimental correlation function, larger lag lengths are calculated with a decreasing amount of data and so the results can become increasingly erratic (see Figure 3.2). Therefore, a choice has to be made on how much of the correlation function should be taken into account when estimating the error. A correlation smaller than -1.0 is theoretically not possible.

Semivariogram
A semivariogram essentially gives the same information as a correlation function (Fenton, 1999). An advantage of the semivariogram is its independence of the estimation of the average value of the soil property (Fenton, 1999). This is a clear advantage because many of the problems of the correlation function relate to this dependence. The sample semivariogram $\hat{V}(\tau_j)$ is defined by:

$$\hat{V}(\tau_j) = \frac{1}{2(n-j)} \sum_{1=1}^{n-j} (x_{i+j} - x_i)^2, \text{ with } j = 0, 1, \ldots, n-1 \quad (3.5)$$

where:
x_i observed value of X_z.
n number of observations in sample of X_z.
j number of lag distances τ.

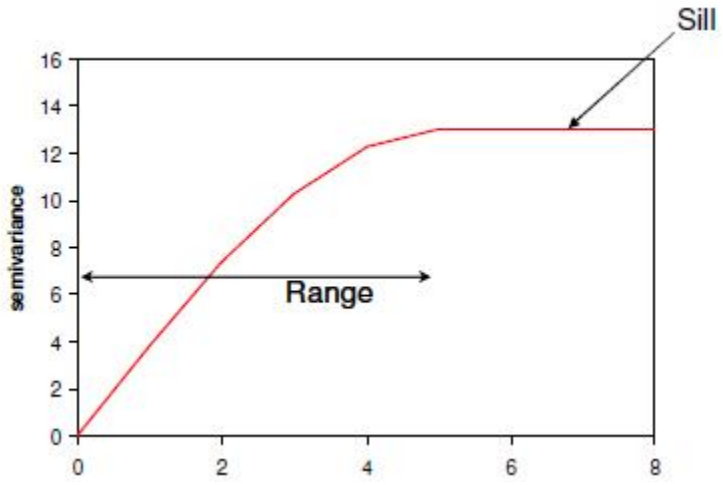

Figure 3.3 Semivariogram with lag distance on the x-axis, range and sill.

Figure 3.3 gives an example of a semivariogram. Range is the distance up till which spatial dependency exists. Sill is the variance around the mean of the observations. This is the maximum semivariance and at this distance no more spatial dependency exists. Another parameter, which is not drawn in the figure, is the nugget. The nugget is an offset of the semivariance which indicates that noise plays a role in the data.
The semivariance can be highly variable. This high variability in the semivariogram may hinder its use in discerning between model types unless sufficient averaging can be performed (Fenton, 1999).

Relation correlation length and variance reduction factor
Vanmarcke (1977) suggested that the variance reduction factor $\Gamma(b)$ can be related to the horizontal correlation length θ by:

$$\Gamma(b) = \left(\frac{\theta}{b}\right)^{1/2} \quad \text{with} \quad b > \theta \tag{3.6}$$

In this equation the variance reduction factor $\Gamma(b)$ depends on the ratio of the horizontal correlation length θ and the length of a potential slip surface b. When applying this equation the horizontal correlation length θ can be easily related to the approach of TAW (2002) and Calle (2007). Note however that the meaning of the variance reduction factor $\Gamma(b)$ is not the same in the approaches of Vanmarcke (1977) and TAW (2002) and Calle (2007). In TAW (2002) and Calle (2007) it is assumed that the variance reduction in vertical direction is nearly complete, whereas the variance reduction in horizontal direction is limited. Vanmarcke (1977) assumes complete averaging of variability in vertical direction and the variance reduction factor decreases when the dimension of a slope failure in horizontal direction increases. When the dimension of a slope failure in horizontal direction is smaller than the correlation length no averaging of variability in horizontal direction occurs according to Vanmarcke (1977).
Vanmarcke (1977) considered that the precise pattern of decay of $\Gamma(b)$ may be rather complex, especially in situations where the spatial variation of strength along a line is attributable to two or more superimposed fluctuations with substantially different correlation length θ. These different types of spatial variation can be modelled as additional sources of uncertainty (Vanmarcke, 1977). In such a model the total variance is the sum of two independent random components, one slow varying and the other rapidly varying, with fractional contributions which add to one. De Gast et al (2017) applied this idea to analyse the

spatial variability in vertical direction using CPT data. They found reasonable results, which are in good agreement with the vertical correlation length as mentioned in TAW (2002).

3.2.2 Spatial variability based on fractal models

Fenton (1999) proposed the fractal model (Figure 3.4). A fractal model seems to fit very well to the character of the natural variability of soil properties. The fractal model implies that different correlation lengths exist on different scales; also on very long scales. This fractal model also follows naturally from the suggestion of Vanmarcke (1977) that the spatial variation of strength along a line may be attributable to two or more superimposed fluctuations with substantially different correlation length θ.

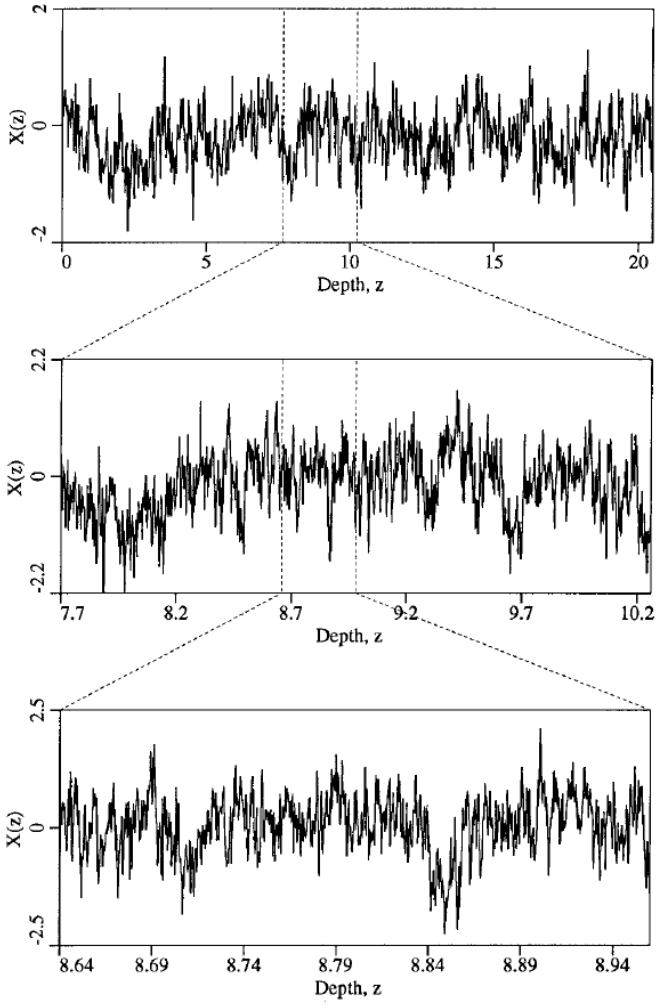

Figure 3.4 Fractal model with recurring pattern of variability according to Fenton (1999). Note that the variability increases when focussing on a smaller depth interval. So the small scale variability averages on the larger scale.

In trying to determine whether the soil property best follows a finite-scale model or a fractal type noise, the periodogram, wavelet variance, and semivariogram plots were found to be the most discriminating by Fenton (1999). In this sense, the periodogram is perhaps the most preferable due to the fact it has been extensively studied. The periodogram and wavelet variance are not investigated in this study.

According to Fenton (1999) there may be little difference between a properly selected finite scale model and the real fractal model over the finite domain.

3.3 Summary

In summary there are two effects to be considered: 1) local variance and regional variance of a soil parameter and 2) averaging of local variance when the scale of the mechanism is larger than the correlation length.

4 Recapitulation results 2017

4.1 Waaldijk Tiel – Waardenburg

Along the Waaldijk between Tiel and Waardenburg a large series of 71 class 1 CPT's is available. This dike section is about 12 km long. The CPT's are carried out by Waterboard Rivierenland (WSRL) in the crest of the dike and in foreshore and hinterland of the dike. These CPT's are analysed in 2017. The focus was on the Holocene clay layer of the Echteld deposits. The most interesting results are presented here very briefly.

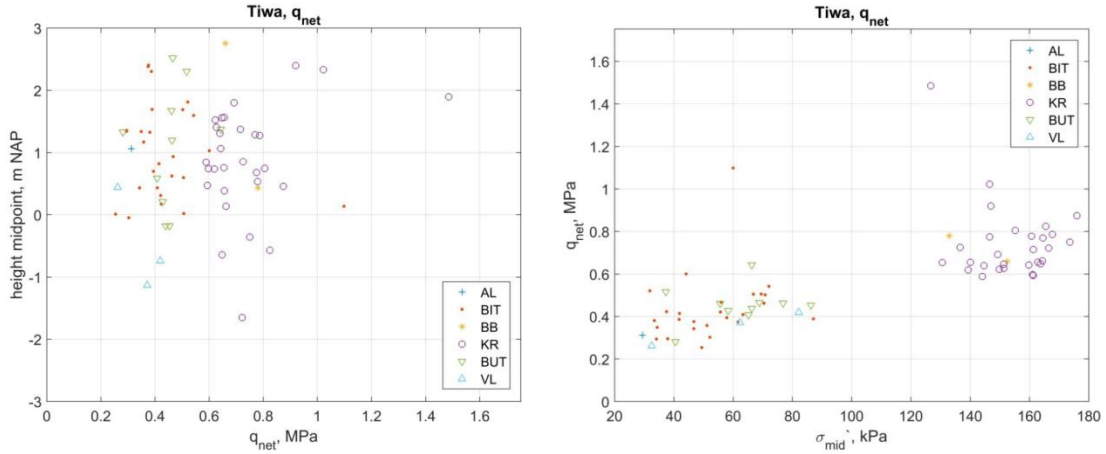

Figure 4.1 Corrected cone resistance q_{net} averaged over the thickness of the soil layer versus height of the midpoint of the concerning CPT (left) and versus vertical effective stress at the midpoint of the concerning CPT (right).

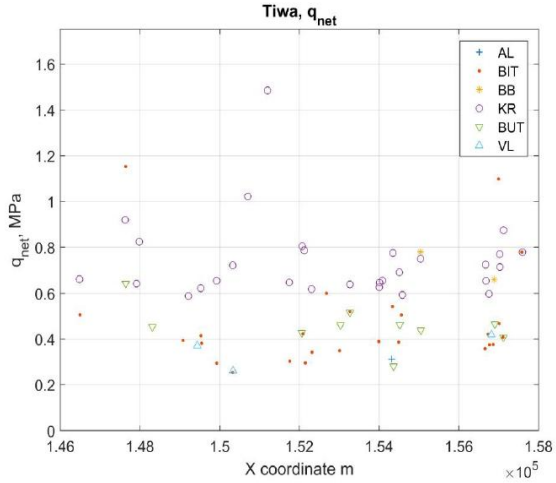

Figure 4.2 Corrected cone resistance q_{net} averaged over the thickness of the soil layer versus x-coordinate of the concerning CPT.

Figure 4.1 (left) shows the corrected cone resistance q_{net} averaged over the thickness of the soil layer on the x-axis and the height of the midpoint of the Echteld layer in the concerning CPT on the y-axis. It can be seen that the bandwidth of the corrected cone resistance is large, but there are clusters of points depending on the location of the CPT's in the hinterland (AL), inner toe (BIT), inner berm (BB), crest (KR), outer toe (BUT) and foreshore (VL). Each of these clusters of points is much smaller than the total bandwidth. The ranges of q_{net} in the

different clusters can be attributed to the effective stresses, which are higher at the crest compared to the other zones. When the corrected cone resistance averaged over the thickness of the soil layer is plotted against the effective stress in the middle of the soil layer a decent trend is visible for most of the clusters (Figure 4.1 right). For each cluster some points are outside of the trend. So it can be seen that the vertical effective stress is an important contribution to the level of the cone resistance. When the corrected cone resistance averaged over the thickness of the soil layer is plotted against the x-coordinate of the CPT no trend can be detected, apart from the effect of the effective stress (Figure 4.2).

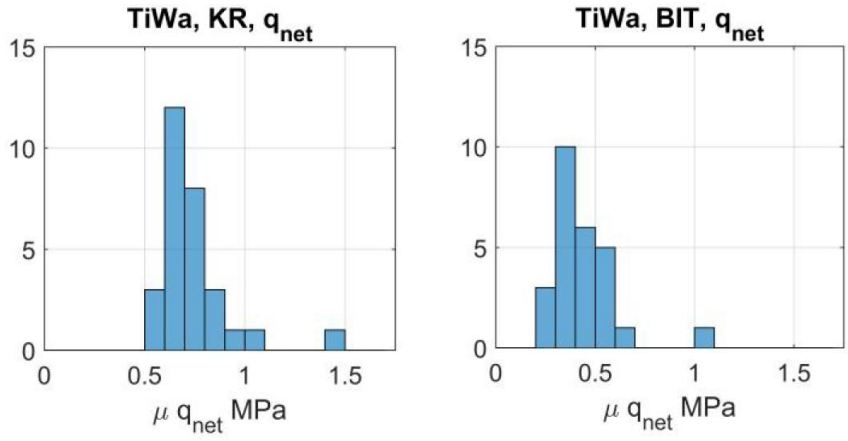

Figure 4.3 Histograms of the corrected cone resistance q_{net} averaged over the thickness of the soil layer; for the crest (left) and the inner toe (right).

The histograms of the corrected cone resistance averaged over the thickness of the soil layer indicate a log-normal distribution of the corrected cone resistance (Figure 4.3).

Location CPT's	Number of CPT's	CoV of the means of all CPT's	Mean CoV per layer per CPT	Median CoV per layer per CPT	Maximum CoV per layer per CPT	Minimum CoV per layer per CPT
Toe, foreshore, hinterland	40	0.32	0.17	0.15	0.43	0.04
Crest	31	0.23	0.15	0.14	0.40	0.05

Table 4.1 Statistics of the corrected cone resistance q_{net} at the Waaldijk.

From Table 4.1 it can be concluded that the variability of the corrected cone resistance q_{net} in vertical direction in a CPT is sometimes very high and sometimes very low, resulting in a factor of about ten between the minimum and maximum CoV. When the variability in a CPT within a soil layer is very high the CoV of the cone resistance of that CPT can be much higher than the CoV of the cone resistance within the soil layer along the whole dike stretch. This local variability within one CPT is thought to average out at the scale of a slip surface of a slope instability. The CoV's per CPT are comparable for the crest and the toe of the dike and foreshore and hinterland. The CoV of the means of the cone resistances of all CPT's together is however larger for the toe, foreshore and hinterland compared to the crest. It is very likely that this can be attributed to the relative larger differences in stress levels at the dike toe and the fore and hinterland.

4.2 Achterwaterschap Alblasserwaard

Along the drainage canals in the western part of the Alblasserwaard also a large series of CPT's is executed by Waterboard Rivierenland (WSRL). 72 class 1 CPT's which are located in the crest of the dike along the drainage canal Achterwaterschap are analysed in 2017. These CPT's are located along a stretch of about 12.5 km. The three research locations with class 1 and class 1+ cones as described in Paragraph 2.1 are situated within this stretch. In this area several Holocene clayey layers from the Echteld Formation and peat from the Nieuwkoop Formation are present in the subsoil.

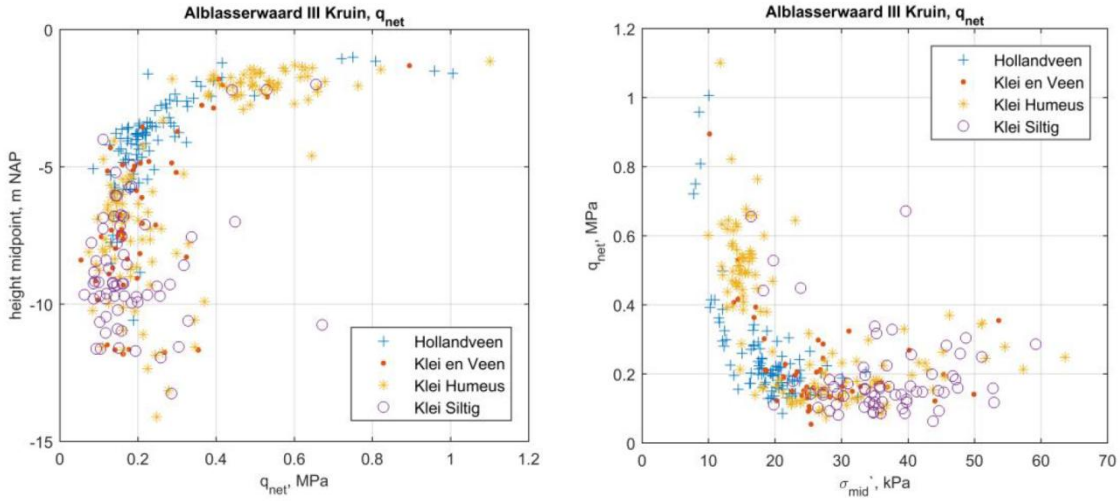

Figure 4.4 Corrected cone resistance q_{net} averaged over the thickness of the soil layer versus height of the midpoint of the concerning CPT (left) and versus vertical effective stress at the midpoint of the concerning CPT (right).

The corrected cone resistance q_{net} averaged over the thickness of the soil layers is presented in Figure 4.4. Figure 4.4 (left) shows the corrected cone resistances against the height of the middle of the soil layer in the concerning CPT's. The most remarkable issue is the difference of the high cone resistances near to the surface compared to the much lower cone resistances at larger depth. It is very likely that the high cone resistances at the surface can be attributed to the interaction with the atmosphere. So the high cone resistance at the surface may be caused by ripening processes. Furthermore the cone resistances of all soil layers are in the same bandwidth. Also when the cone resistance is plotted against the vertical effective stress in the middle of the soil layer in the concerning CPT's the difference between the firm crust and the deeper layers is remarkable (Figure 4.4 right). The stress dependency is not clear in the deeper soil layers. Only the humic clay (yellow stars; 'Klei humeus' in Dutch) show some increase in cone resistance for increasing effective stress.

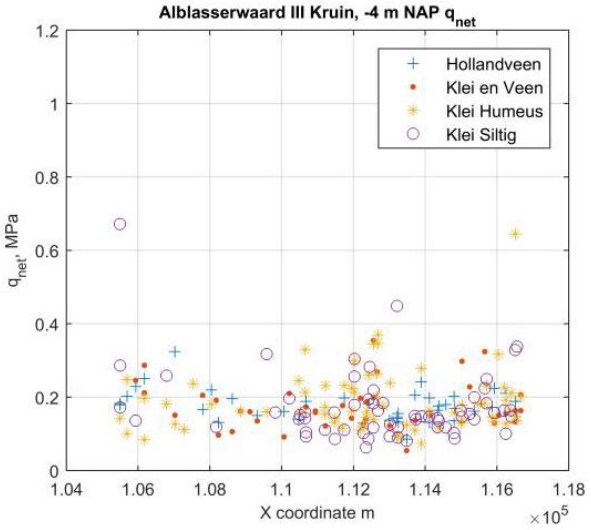

Figure 4.5 Corrected cone resistance q_{net} averaged over the thickness of the soil layer versus x-coordinate of the concerning CPT.

When de corrected cone resistance is plotted against the x-coordinate of the locations of the CPT's no trend can be found (Figure 4.5).

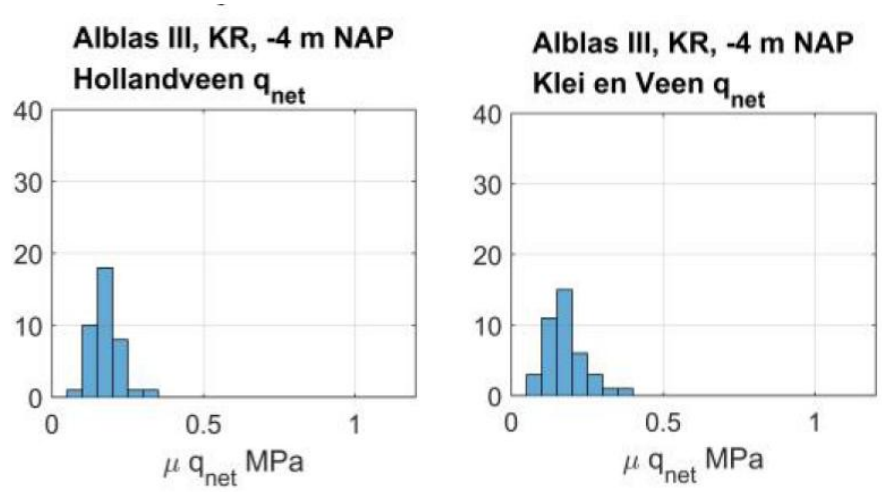

Figure 4.6 Histograms of the corrected cone resistance q_{net} averaged over the thickness of the soil layer; for peat (left) and peaty clay (right).

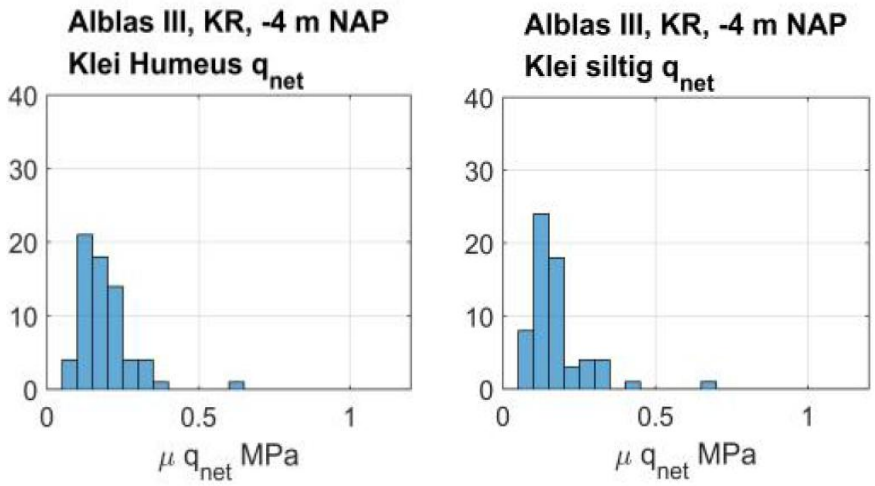

Figure 4.7 Histograms of the corrected cone resistance q_{net} averaged over the thickness of the soil layer; for humic clay (left) and clay (right).

As found for the Echteld clay layer at the Waaldijk in Paragraph 4.1 also the averaged corrected cone resistance q_{net} of the soil layers at the Achterwaterschap show a log-normal distribution (Figure 4.6 and Figure 4.7).

Soil layer	Number of CPT's	Mean q_{net} (MPa)	Standard deviation q_{net} (MPa)	CoV of the means of CPT's
Peat	39	0.18	0.04	0.24
Clay and peat	40	0.18	0.06	0.36
Clay humic	67	0.19	0.09	0.46
Clay	63	0.17	0.10	0.56

Table 4.2 Statistics of the corrected cone resistance q_{net} at the Achterwaterschap.

Some statistics of the averaged corrected cone resistance of the soil layers at the Achterwaterschap are summarized in Table 4.2. These statistical data will be used in the analysis in Paragraph 5.5.

Soil layer	Number of CPT's	CoV of the means of all CPT's	Mean CoV per layer per CPT	Median CoV per layer per CPT	Maximum CoV per layer per CPT	Minimum CoV per layer per CPT
Peat	39	0.24	0.29	0.21	1.49	0.02
Clay and peat	40	0.36	0.34	0.28	1.05	0.11
Clay humic	67	0.46	0.32	0.23	1.35	0.01
Clay	63	0.56	0.20	0.15	1.05	0.02

Table 4.3 Statistics of the corrected cone resistance q_{net} at the Achterwaterschap.

Compared to the Waaldijk more or less the same can be seen for the CPT data of the Achterwaterschap in Table 4.3. Again there is a large range in CoV's of the corrected cone resistance in vertical direction in the CPT's, where this CoV can be very small but also very large and also much larger than the CoV of the means of all CPT's together. At the Waaldijk

the ratio between the minimum and maximum CoV of the CPT's was a factor of about ten, but this factor is much more at the Achterwaterschap. The corrected cone resistances at the Achterwaterschap are sometimes very low, which partly can explain the high CoV's. Remarkable high is the minimum CoV of the peaty clay layer, which a value 0.11 much higher than other layers. The CoV of the means of the cone resistances of all CPT's together is more or less in the same range as the Waaldijk. Note that only CPT's at the crest are analysed.

4.3 Balgzanddijk and Amsteldiepdijk

At the south east of Den Helder are the Balgzanddijk and Amsteldiepdijk. These dikes belong to the administration of Hoogheemraadschap Hollands Noorderkwartier. Along these dikes 30 class 2 CPT's are available in the crest and the inner berm. In this area the Holocene deposits are from the Naaldwijk Formation. The deposits of interest are different types of marine clay and peat (Nieuwkoop Formation).

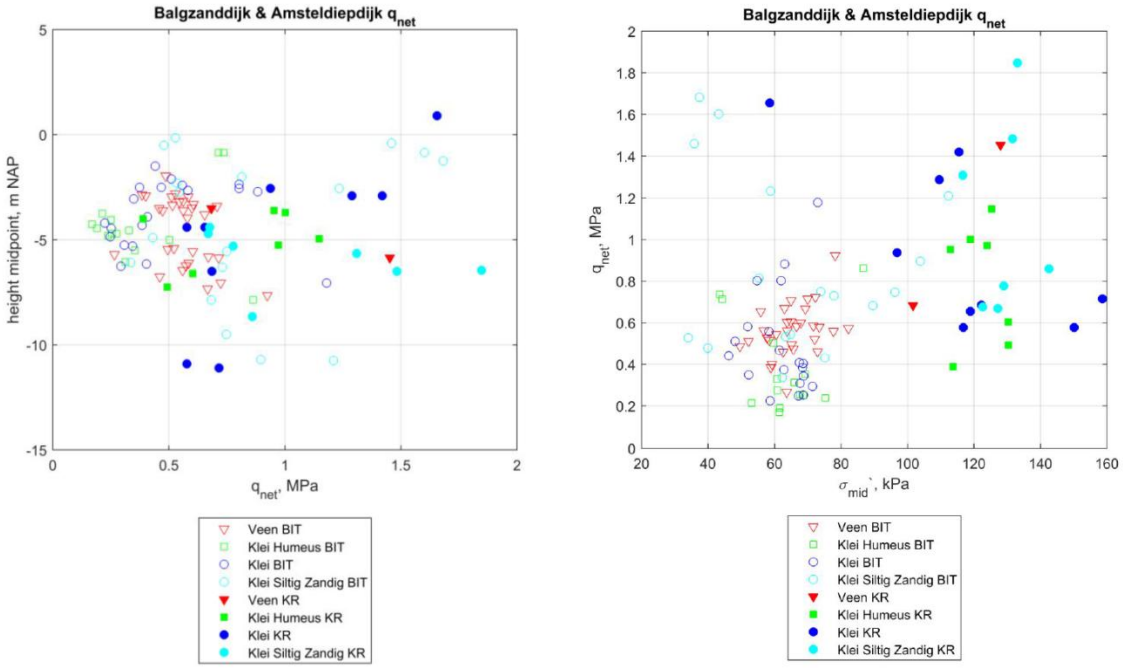

Figure 4.8 Corrected cone resistance q_{net} averaged over the thickness of the soil layer versus height of the midpoint of the concerning CPT (left) and versus vertical effective stress at the midpoint of the concerning CPT (right).

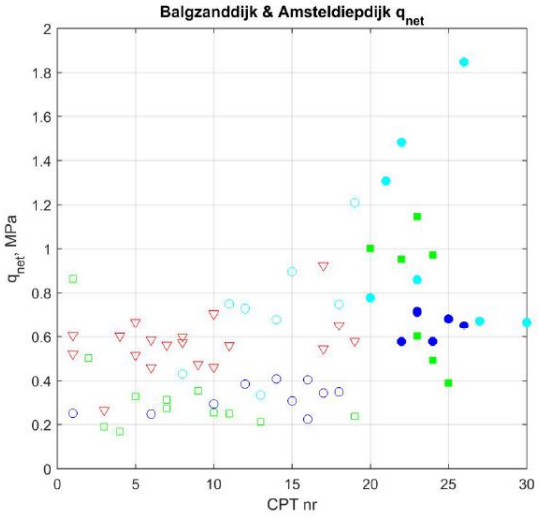

Figure 4.9 Corrected cone resistance q_{net} averaged over the thickness of the soil layer versus number of the concerning CPT.

Figure 4.8 (left) shows the corrected cone resistance averaged over the thickness of the soil layers versus the height of the midpoint of the soil layer in the concerning CPT's. The corrected cone resistance averaged over the thickness of the soil layers versus the vertical effective stress at the midpoint of the soil layer in the concerning CPT's is presented in Figure 4.8 (right). Both figures show much scatter; no trends can be recognized. The CPT's 1 to 21 are located at the inner berm and CPT's 22 to 30 are located at the crest (Figure 4.9). The cone resistances at the crest of the dike (KR) are on average somewhat higher than the cone resistances at the inner berm (BIT), which can be attributed to the higher stress level at the crest of the dike. Furthermore the cone resistance of all soil layers is in the same range without a trend along the dike section.

Soil layer	Number of CPT's	CoV of the means of all CPT's	Mean CoV per layer per CPT	Median CoV per layer per CPT	Maximum CoV per layer per CPT	Minimum CoV per layer per CPT
Peat (b)	19	0.22	0.10	0.10	0.18	0.01
Peat (c)	--	--	--	--	--	--
Clay humic (b)	12	0.58	0.27	0.24	0.67	0.05
Clay humic (c)	7	0.37	0.26	0.09	0.59	0.05
Clay (b)	10	0.21	0.16	0.09	0.37	0.04
Clay (c)	5	0.10	0.13	0.12	0.24	0.05
Sandy clay (b)	8	0.37	0.38	0.38	0.57	0.20
Sandy clay (c)	7	0.42	0.37	0.38	0.44	0.25

Table 4.4 Statistics of the corrected cone resistance q_{net} at the Balgzanddijk and Amsteldiepdijk; (b) = inner berm and (c) = crest

Compared to the Waaldijk and the Achterwaterschap similar trends can be observed at the Balgzanddijk and Amsteldiepdijk (Table 4.4). At the Balgzanddijk and Amsteldiepdijk the sandy clay layer is relatively very variable because the minimum CoV of a CPT is 0.20. This can be caused by the variable drainage conditions in the sandy clay during penetration of the CPT's. For the peat layer the maximum CoV per CPT is equal to the CoV of the means of all CPT's together.

4.4 Summary

Important differences in cone penetration resistances are encountered in the analyses of the dike sections as described in this chapter. These differences appear in the mean values as well as in the variability of the cone penetration resistances. It is very likely that these differences can be attributed to the differences in depositional environments and stress history of the soil.

The variability of the cone penetration resistances in the dike section of the Waaldijk between Tiel and Waardenburg is relatively small compared to the results of both other locations. The cone penetration resistances from the dike section Tiel – Waardenburg also show a nice relationship with effective vertical stress. In both other locations this relationship is absent.

In all dike sections and soil types the distribution of the cone penetration resistance seems to be a log-normal distribution. Trends in the mean values of the cone penetration resistances along the dike sections could not be identified.

5 Results Achterwaterschap

5.1 Stratigraphy derived from CPT data

The measured cone penetration resistances q_c from the class 1 and class 1+ cones at the three investigated locations along the "Achterwaterschap" are given in Figure 5.1, Figure 5.2 and Figure 5.3.

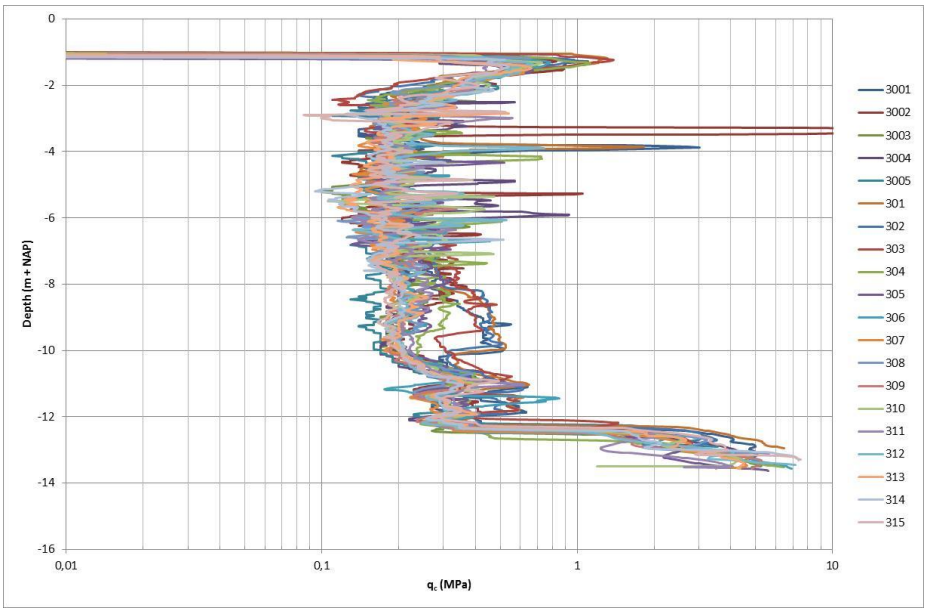

Figure 5.1 Measured cone penetration resistance q_c at location AC 075

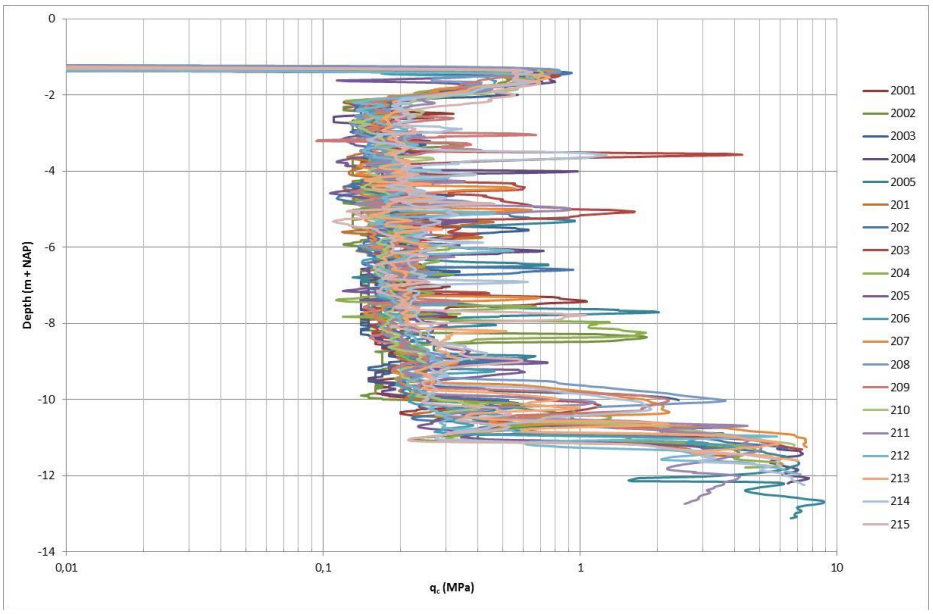

Figure 5.2 Measured cone penetration resistance q_c at location AC 090

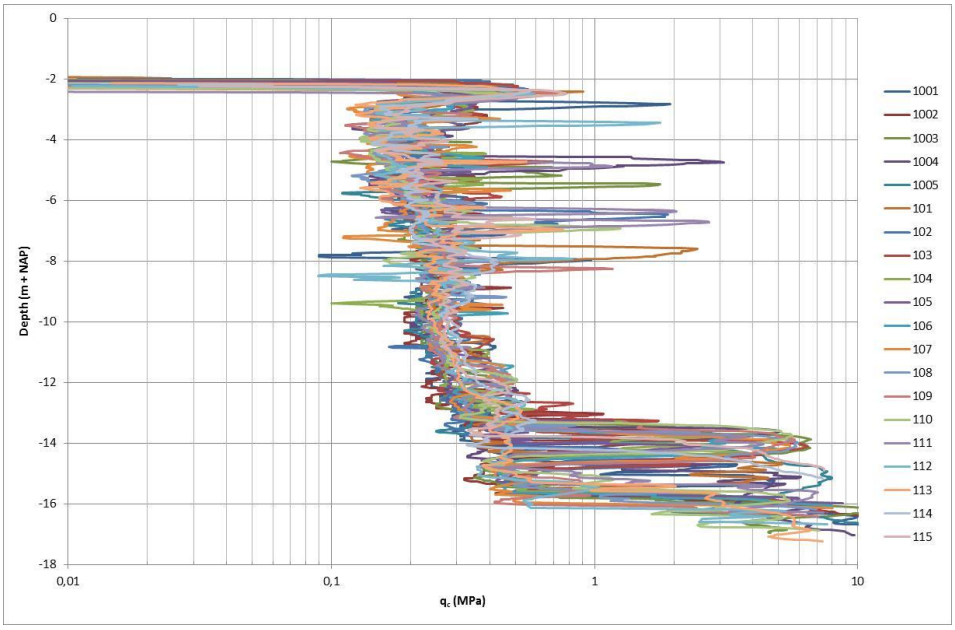

Figure 5.3 Measured cone penetration resistance q_c at location AC 251

The figures show the variability of the measured cone penetration resistances q_c. In general, the q_c values show consistent results. The top of the firm Pleistocene sand layers can be found between NAP -11 m and NAP -16 m. The Holocene layers show a measured cone penetration resistance between 0.15 and 0.4 MPa. In the top layer near the surface higher cone resistances of about 0.8 MPa are measured. Roughly the cone penetration resistances at the three sites are in the same order of magnitude.

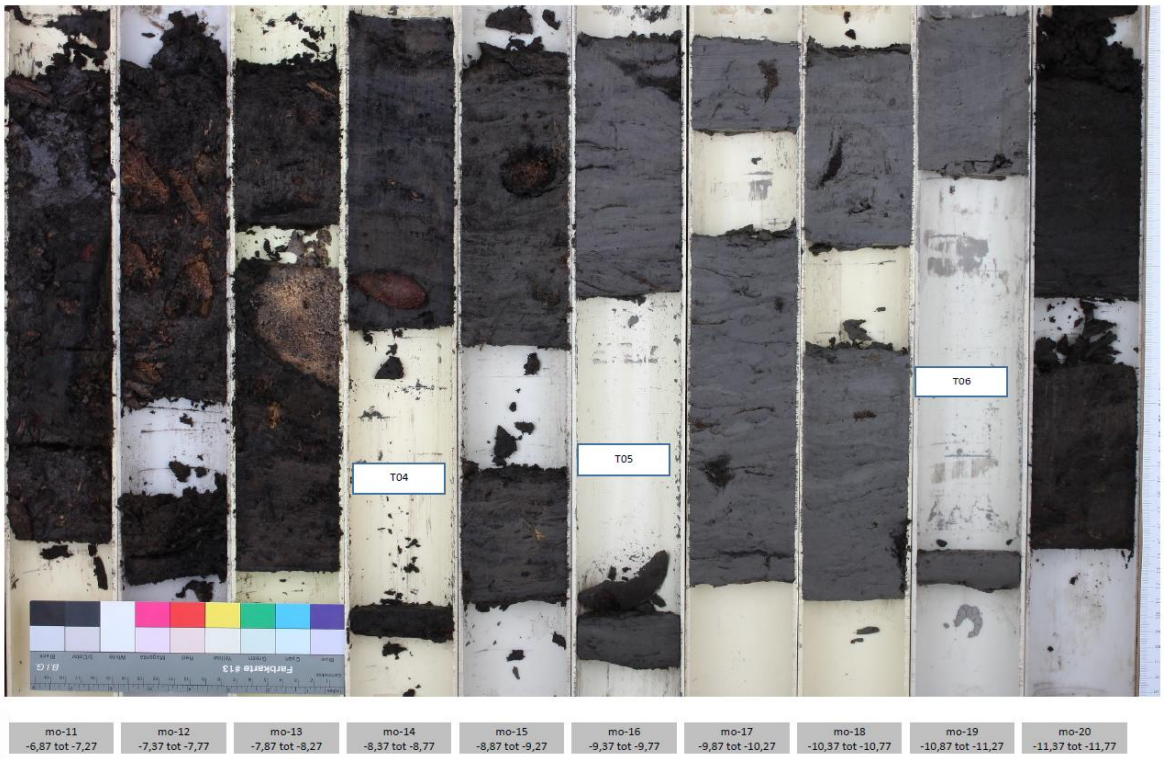

Figure 5.4 Photo of samples from bore hole B-100 at location AC 251 with fragments of wood in peat and humic clay

Figure 5.1, Figure 5.2 and Figure 5.3 show several spikes in the measured cone penetration resistances in the soft Holocene layers (between NAP -2 and -10 m), which can be attributed to fragments of wood in peat and humic clay. These fragments of wood can be recognized in the photo of the samples from bore hole B-100 at location AC 251 (Figure 5.4). Spikes are ignored in the analysis of the variability of the cone penetration resistance, which is a conservative choice given that the spikes are an increase in cone penetration resistance, but due to the limited scale of the fragments, this is not deemed sufficient to derive strength from.

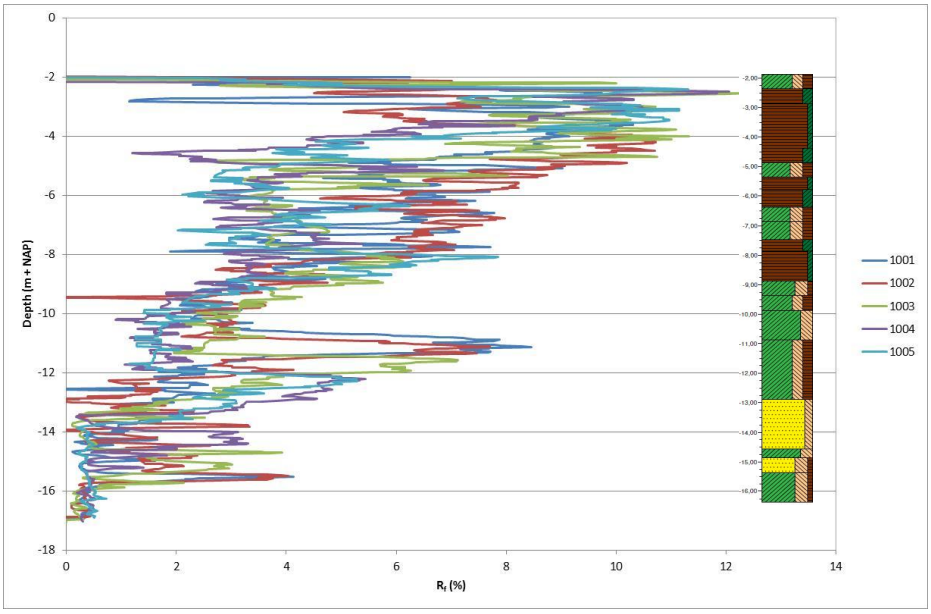

Figure 5.5 Begemann classification at location AC 251 and bore hole B-100

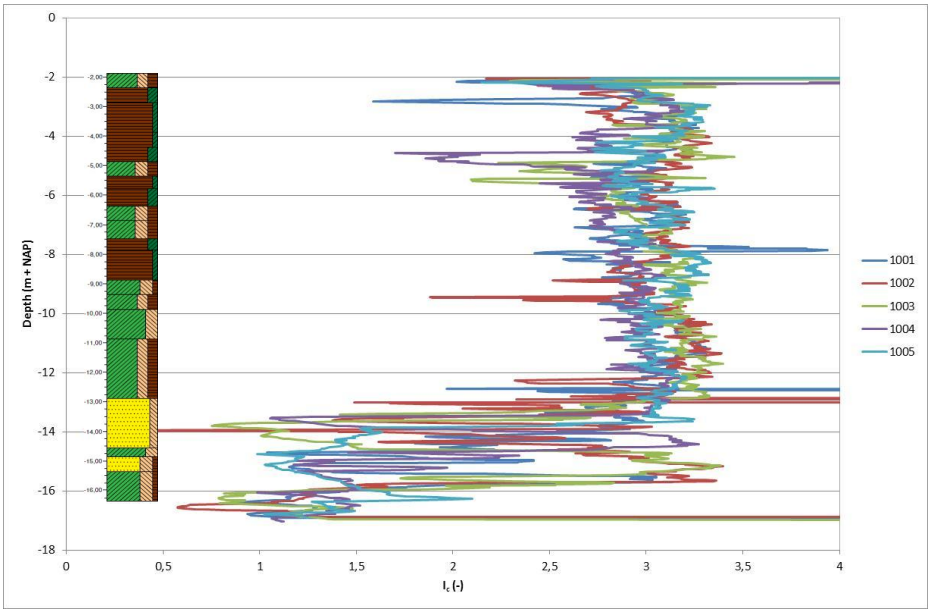

Figure 5.6 Jefferies and Been classification at location AC 251 and bore hole B-100

When applying the Begemann and Been and Jefferies classification systems it turns out that the Begemann classification system is more appropriate for Dutch humic soils than the Jefferies and Been classification. The Jefferies and Been classification classifies most of the soil layers in the same category (I_c > 2.9) as illustrated in Figure 5.6. The Begemann

classification results in an increasing friction ratio in upward direction. This trend fits well to the soil description as derived from bore hole B-100 (Figure 5.5).

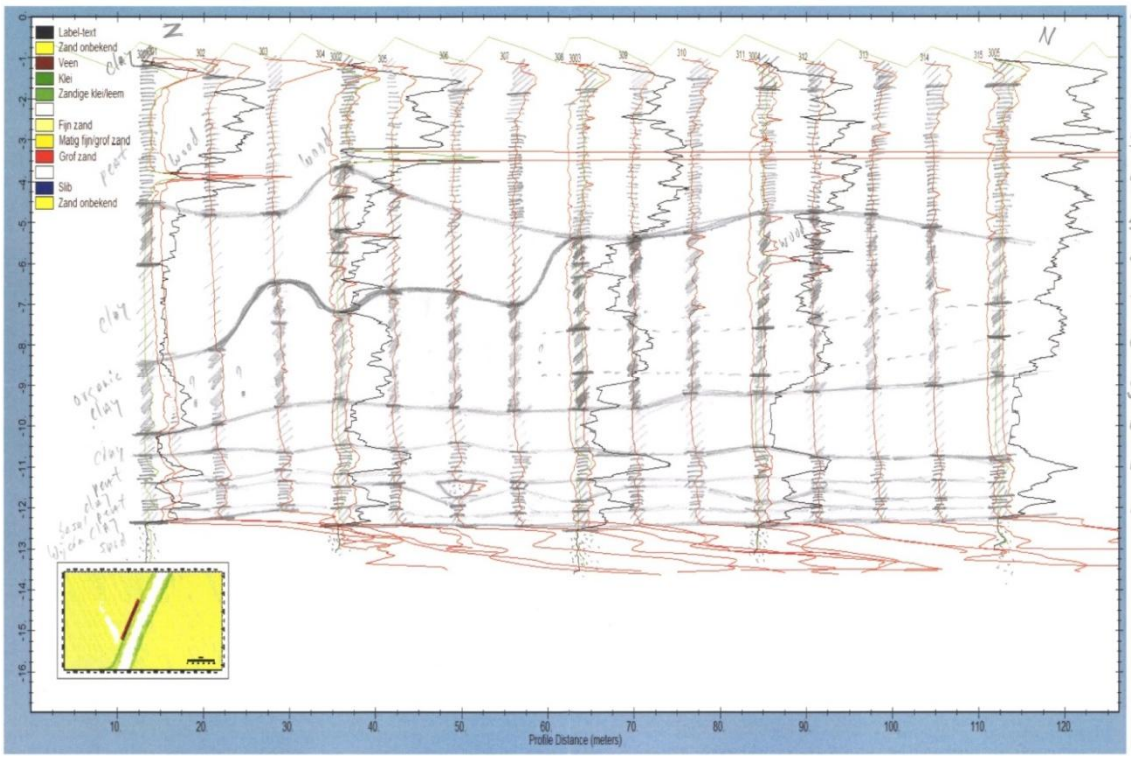

Figure 5.7 Interpreted stratigraphy at location AC 075

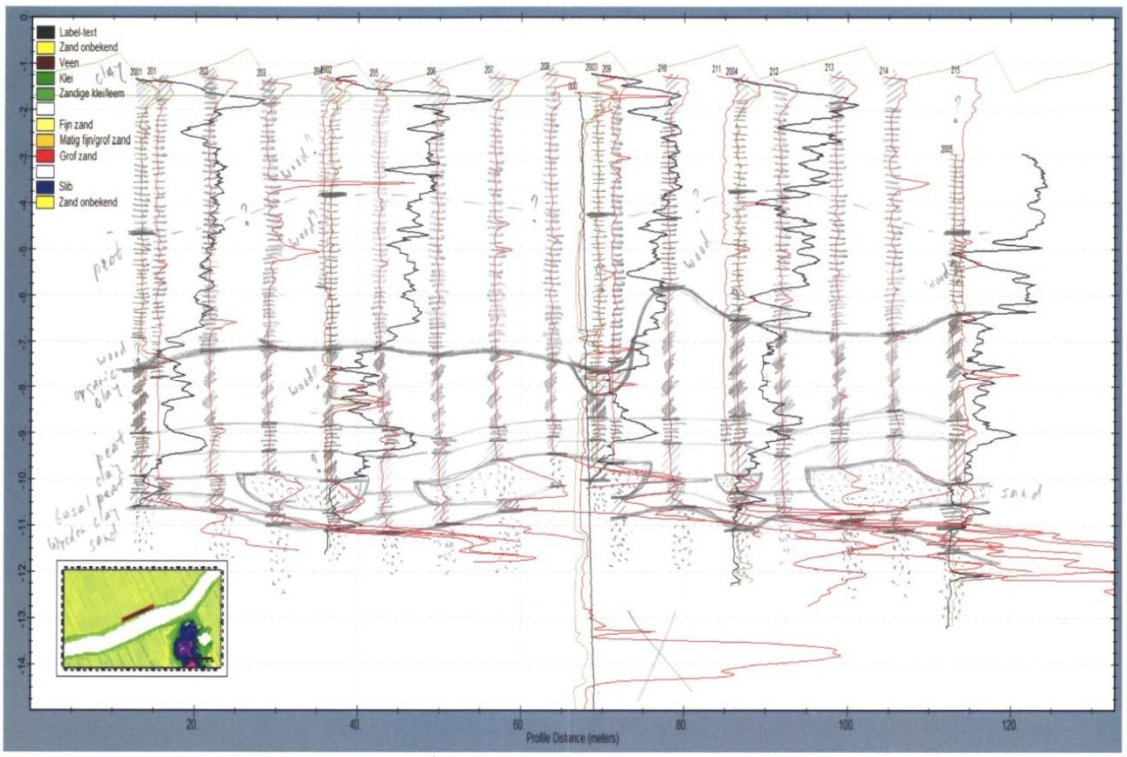

Figure 5.8 Interpreted stratigraphy at location AC 090

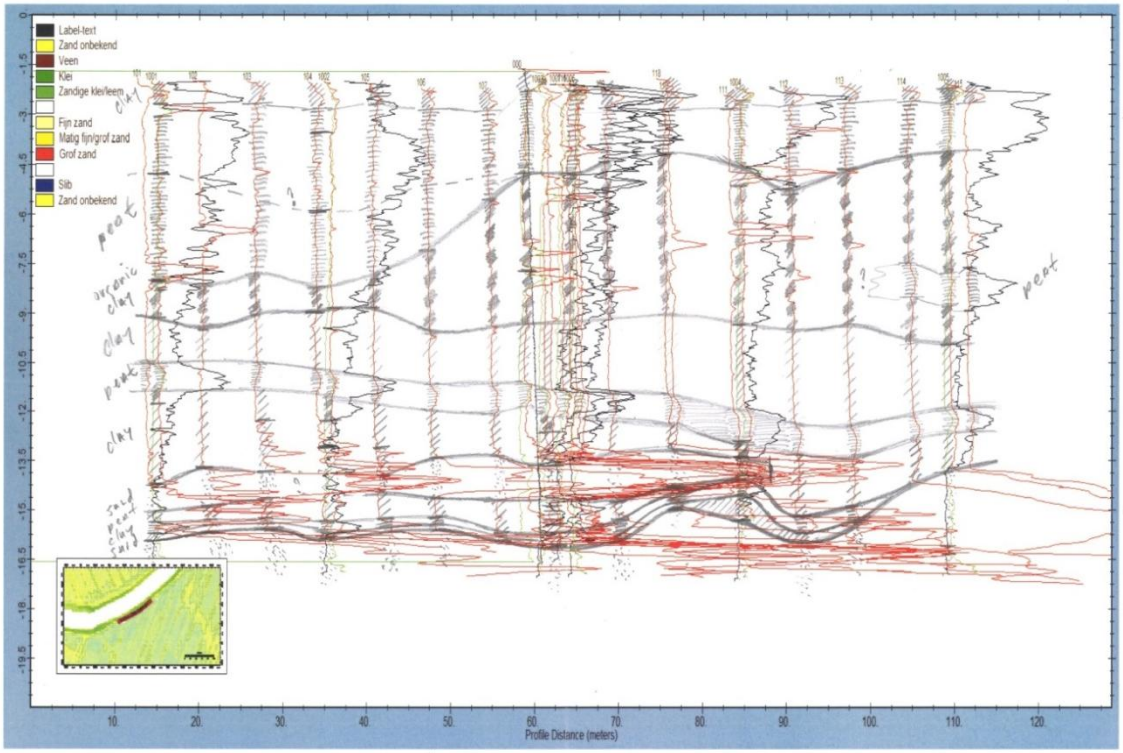

Figure 5.9 Interpreted stratigraphy at location AC 251

Figure 5.7, Figure 5.8 and Figure 5.9 show the interpreted stratigraphy of the three locations. As mentioned before the top of the firm Pleistocene sand layers can be found between NAP -11 m and NAP -16 m. The depth of the top of the Pleistocene sand layers increases from east to west. At location AC 251 the top of the Pleistocene sand layer shows a lot of relief. On top of the Pleistocene sand layer the flood basin deposits of the Wijchen Member can be recognized. The thickness of this layer is between some decimetres and about one meter. Basal peat has been formed on top of the Wijchen Member. Channel belt deposits from the Echteld Formation can be derived from the data below NAP -9.5 m. These channel belt deposits are very thin with only one sandy channel at location AC 075. At both other locations the channel belt deposits are much thicker. At AC 090 four sandy channels with varying dimensions can be derived from the CPT data. The channels partly eroded the Basal peat and Wijchen Member. Above the channel belt deposits the subsoil is dominated by humic and peaty clay, which are floodbasin deposits from the Echteld Formation, and peat from the Nieuwkoop Formation. The peat layers can be divided in eutrophic peat and mesotrophic peat The top of the eutrophic peat is around NAP -4 m to NAP -5 m. This stratigraphy is in good agreement with the stratigraphy as described by Gouw et al (2007) and Hijma et al (2009).

Analysing the results of the class 1+ cones it proves that the interpretation of these results is difficult because the pore water pressure u_2 and sleeve friction f_s were not measured. Only the cone penetration resistance is not sufficient to make accurate decisions on boundaries between soil layers. Pore water pressure and sleeve friction offer useful additional information for the soil classification. The measurements of the class 1 cones sometimes show an alternation of peaty and humic layers. Examples are location AC 075 at NAP -7 m to NAP -10 m and location AC 251 around NAP -8 m. The boundary between eutrophic peat and mesotrophic peat can not be determined from the results of the class 1+ cones. It can be expected that these uncertainties will cause scatter in the analysis as discussed in the next paragraphs.

5.2 Correction and normalization of CPT data

When the stratigraphy has been determined, soil unit weights can be ascribed to the soil layers and stationary pore water pressures can be schematized. With this additional information the corrected cone penetration resistance q_{net} and normalized cone penetration resistance Q_t can be calculated according to equations 2.1, 2.2 and 2.3. It has to be noted that not much is known about the phreatic level. The schematization of the stationary pore water distribution is based on the measurements of the pore water pressure during cone penetration (class 1 cone). The variation of the soil unit weight is also uncertain. So uncertainty is introduced in the analyses due to the corrections and normalization.

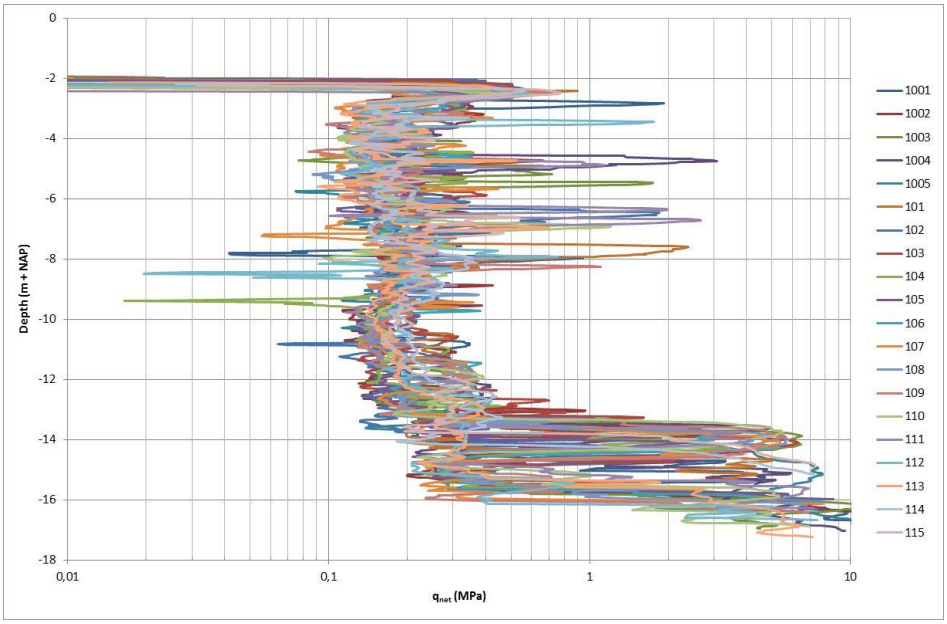

Figure 5.10 Corrected cone penetration resistance q_{net} at location AC 251

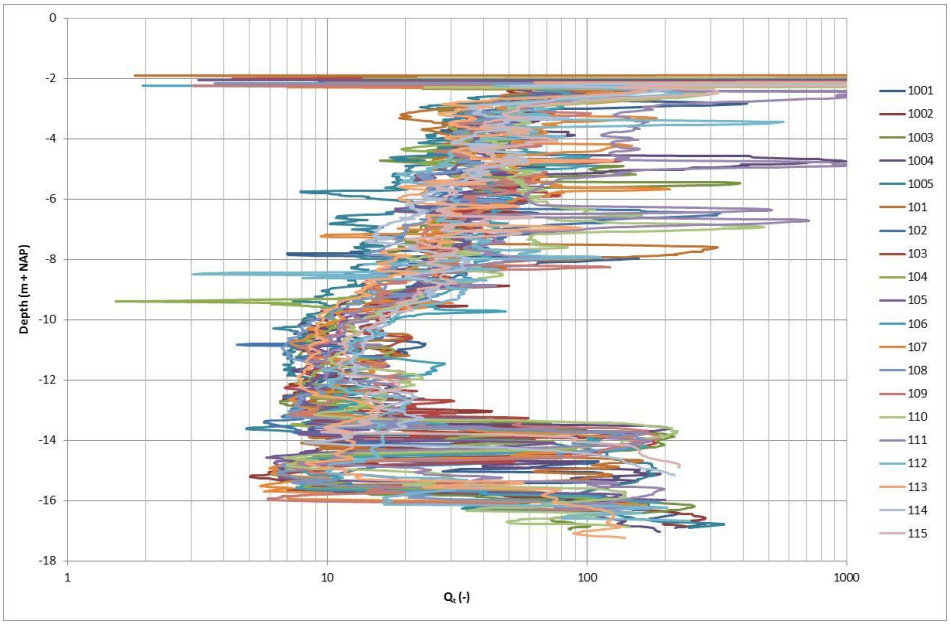

Figure 5.11 Normalized dimensionless cone penetration resistance Q_t at location AC 251

The corrected cone penetration resistance at location AC 251 is showed in Figure 5.10. The normalized cone penetration resistance is given in Figure 5.11. When comparing these figures with the measured cone penetration resistance as shown in Figure 5.3 the impact of the corrections and normalisation can be observed. The corrected cone penetration resistance is substantially lower (~40 - 50%) than the measured cone penetration resistance because of the corrections for measured pore water pressure and total vertical stress. This relatively large effect of the corrections is caused by the low measured cone penetration resistances. By normalising the corrected cone penetration resistance, the pattern of the CPT data changes. This normalisation is required because the stratigraphy as derived from the CPT's is not constant and some layers are not horizontal, as can be seen in Figure 5.7, Figure 5.8 and Figure 5.9; so the vertical effective stresses will be different at each CPT.

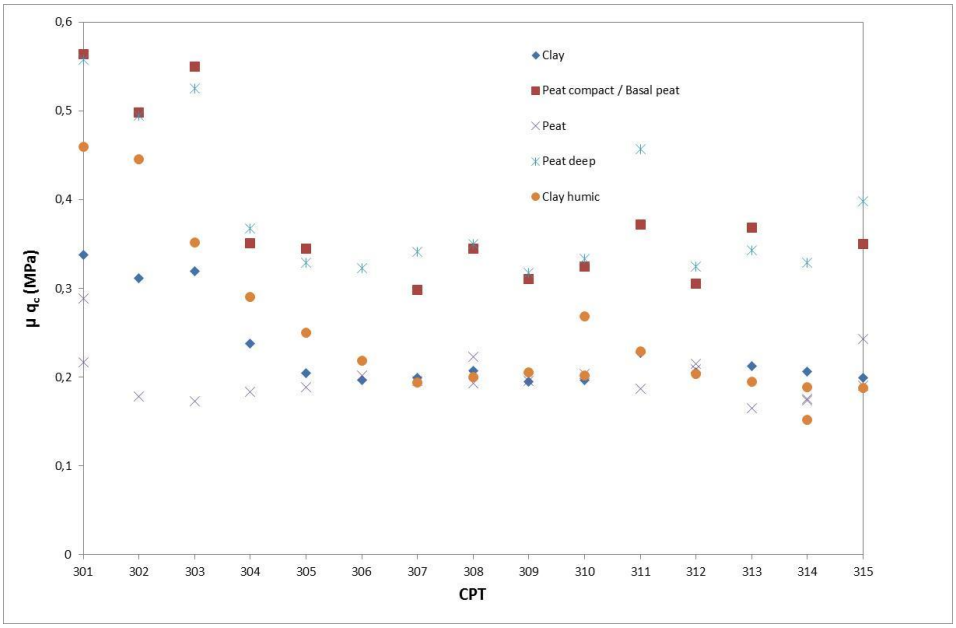

Figure 5.12 Measured cone penetration resistance q_c per soil layer at location AC 075

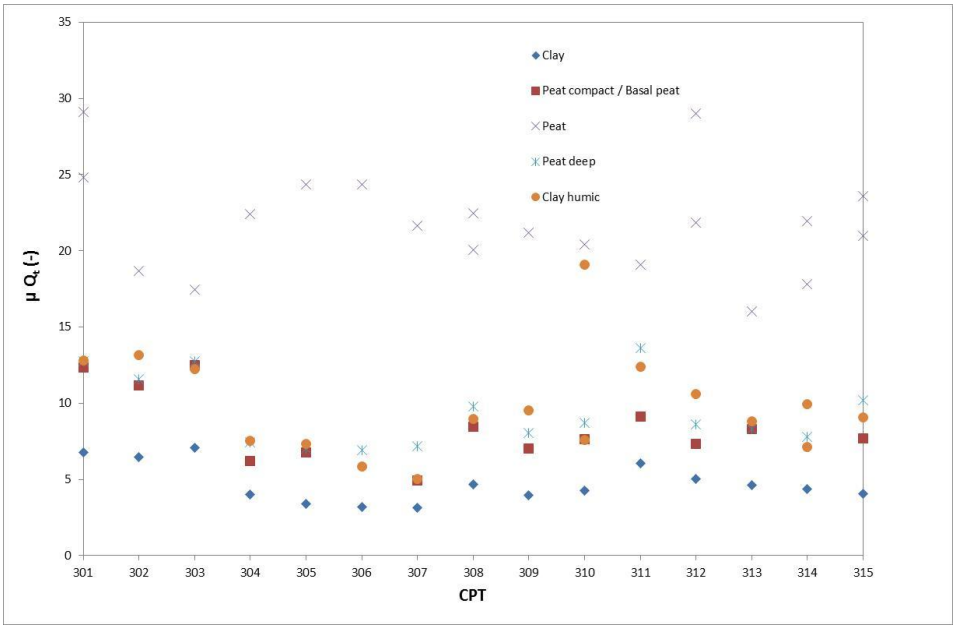

Figure 5.13 Normalized dimensionless cone penetration resistance Q_t per soil layer at location AC 075

Figure 5.12 and Figure 5.13 also illustrate the effect of the applied corrections and normalisation. For each CPT the cone penetration resistances are averaged over the thickness of the soil layers. The figures show the corrections and normalisation for the CPT data from location AC 075. At this location the stratigraphy varies because the thickness of the soil layers varies, as can be seen in Figure 5.7. Due to the corrections and normalisation the trends in Figure 5.13 differ from the trends in Figure 5.12, however, the magnitude of the variability is more or less the same. The normalized cone penetration resistance Q_t in Figure 5.13 shows some jumps, for example between CPT 303 and CPT 304 and between CPT 307 and CPT 308. When Figure 5.13 is compared with Figure 5.7 these jumps can be related to changes in the stratigraphy.

5.3 Variability cone penetration resistance

In order to quantify the variability of the cone penetration resistance mean values and standard deviations of the CPT data are calculated.

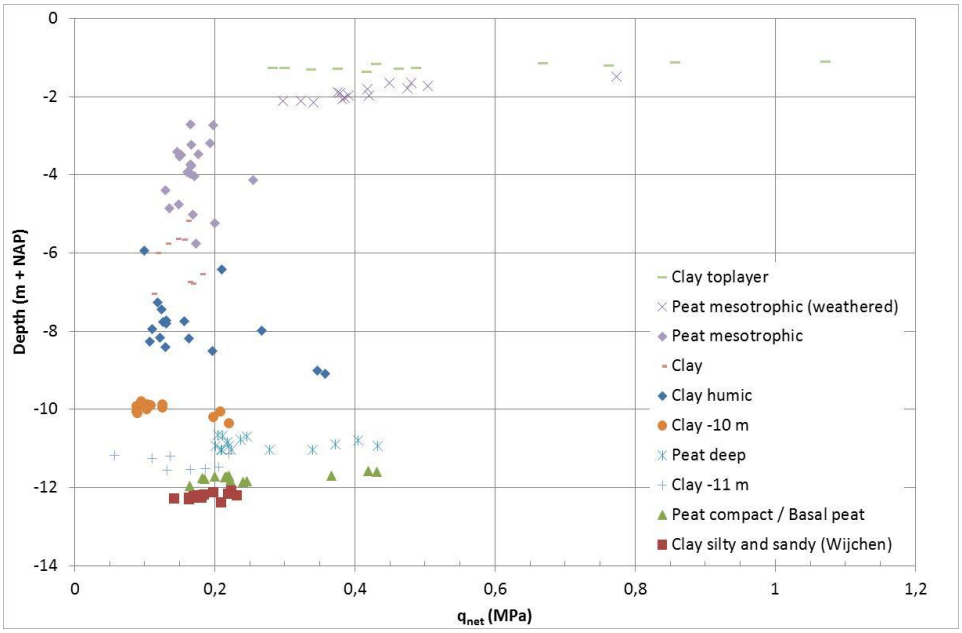

Figure 5.14 Variability of the corrected cone penetration resistance q_{net} at location AC 075

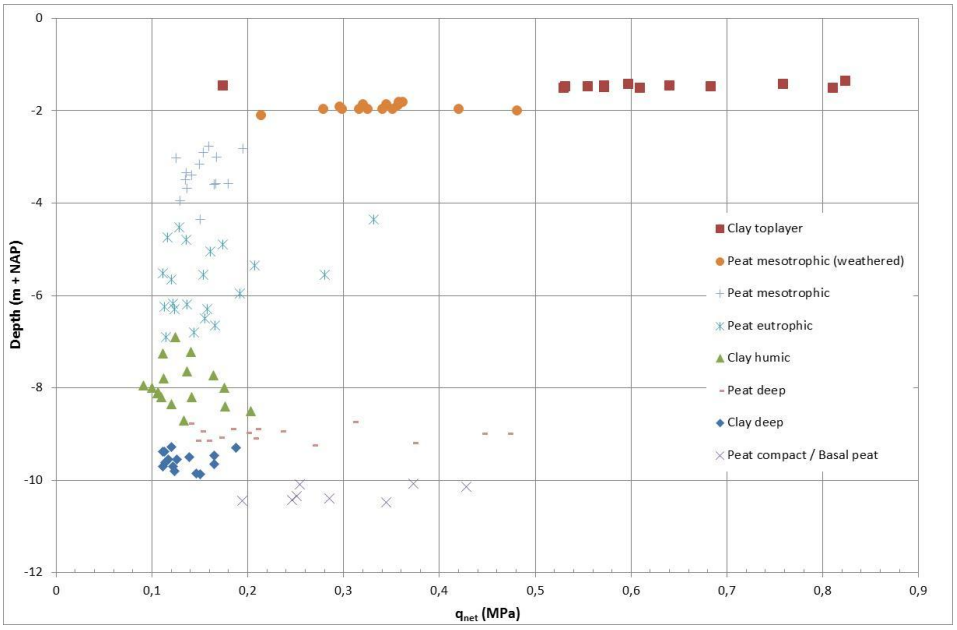

Figure 5.15 Variability of the corrected cone penetration resistance q_{net} at location AC 090

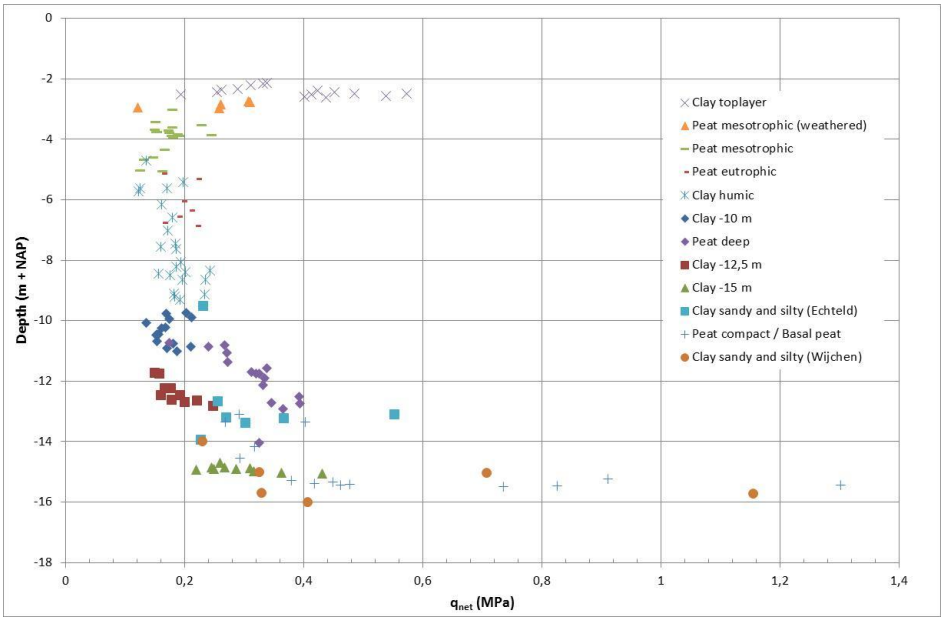

Figure 5.16 Variability of the corrected cone penetration resistance q_{net} at location AC 251

Figure 5.14, Figure 5.15 and Figure 5.16 show the variability of the corrected cone resistance per location. For each location, the calculated mean values of the corrected cone resistances per soil layer and per CPT are presented at the depth of the middle of the concerning soil layer. First of all the stiff top layer can be recognized. Furthermore it can be seen that the middle of the soil layers varies enormously, meaning that the soil layers are not horizontal and vary in thickness. The variability of the cone resistance is largest for the deep peat layers. This variability can be caused by variations in shear strength, variations in drainage conditions during cone penetration. Also the fact that these deep peat layers are relatively thin may play a role. The mean values of the cone resistances of these peat layers are based on a limited number of measurement values. Overall the ratio between the high cone resistances and low cone resistances per soil layer is about 2 or 3.

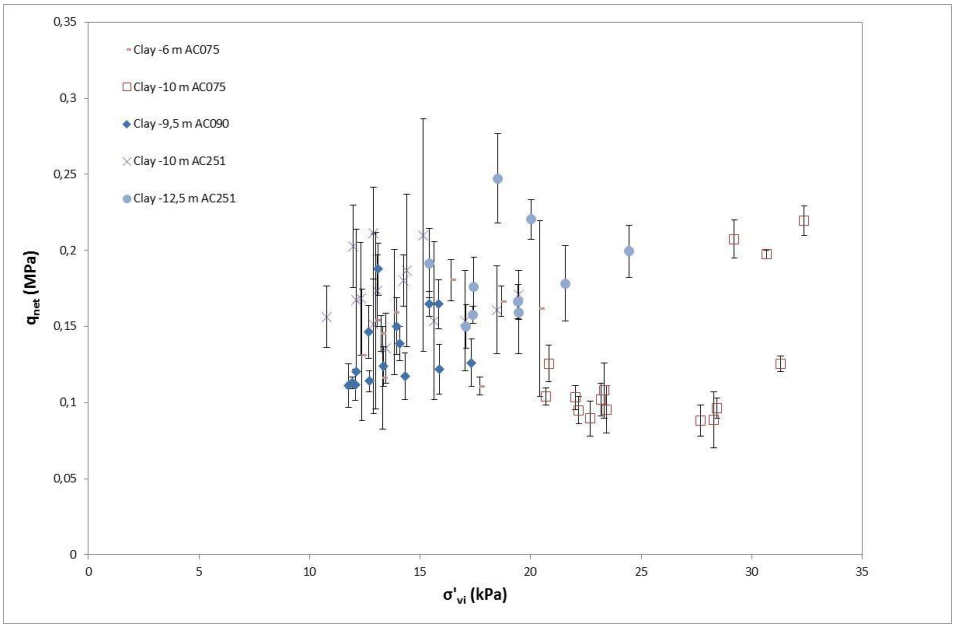

Figure 5.17 Variability of the corrected cone penetration resistance q_{net} of clays

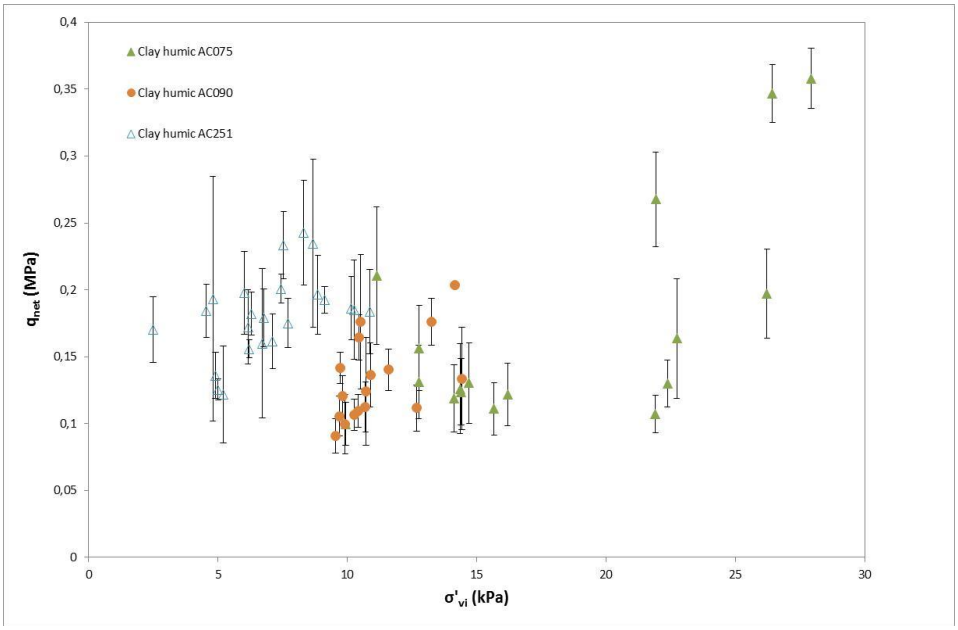

Figure 5.18 Variability of the corrected cone penetration resistance q_{net} of humic clays

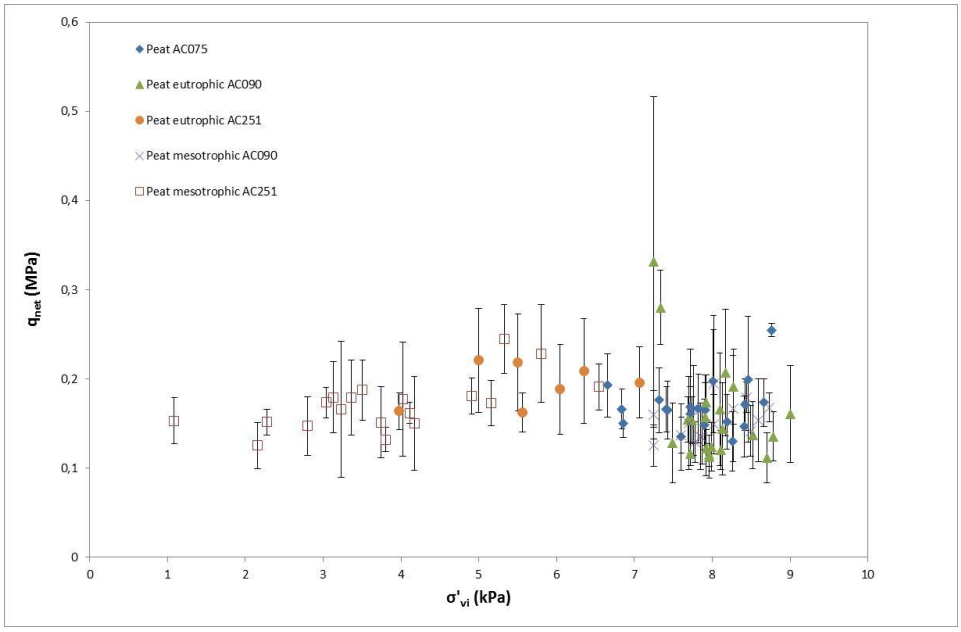

Figure 5.19 Variability of the corrected cone penetration resistance q_{net} of peat

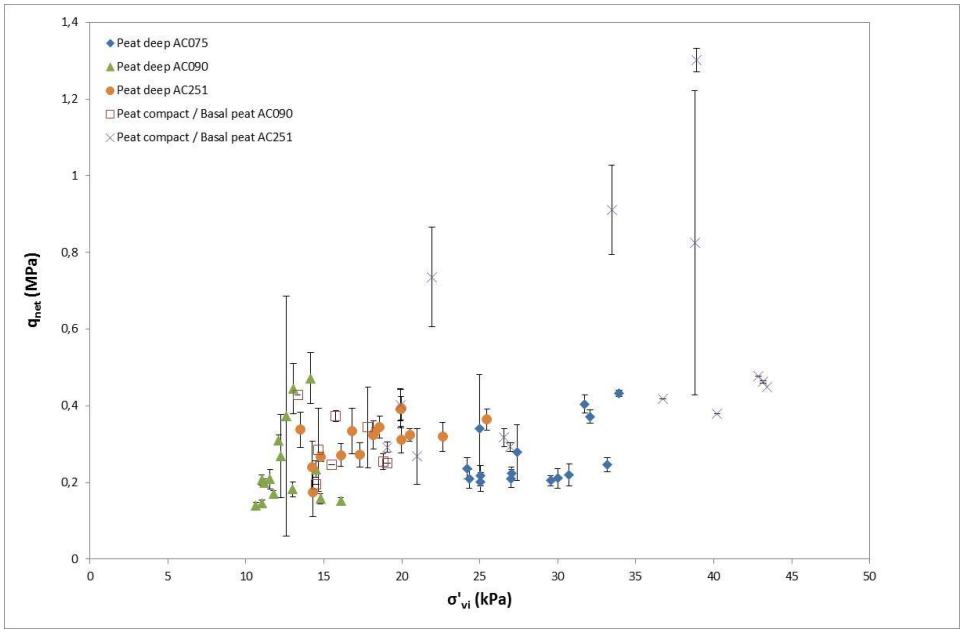

Figure 5.20 Variability of the corrected cone penetration resistance q_{net} of peat

Figure 5.17, Figure 5.18, Figure 5.19 and Figure 5.20 again show the variability of the cone resistance. In these figures the corrected cone resistance q_{net} versus the vertical effective stress is plotted per soil type. Each symbol represents the mean value of the corrected cone resistance of the concerning soil layer within one CPT. At each symbol the 90% confidence interval is given. The figures show a lot of differences. In all soil layers there is a lot of variability in mean values of the cone resistances, the 90% confidence interval and the effective stress level. A clear stress dependency of the cone penetration resistance can not be identified.

Soil type	Loc-ation	CPT's with class 1+ cone					CPTu's with class 1 cone				
		n (-)	μ q_{net} (MPa)	σ q_{net} (MPa)	σ^2 q_{net} (MPa)	CoV q_{net} (-)	n (-)	μ q_{net} (MPa)	σ q_{net} (MPa)	σ^2 q_{net} (MPa)	CoV q_{net} (-)
Clay -10 m	AC075	15	0.123	0.046	0.0021	0.371	5	0.131	0.064	0.0041	0.490
Clay -10 m	AC251	15	0.172	0.022	0.0005	0.130	5	0.159	0.005	0.0000	0.034
Clay -11 m	AC075	8	0.152	0.054	0.0029	0.354	4	0.250	0.147	0.0216	0.588
Clay -12,5 m	AC251	10	0.185	0.031	0.0009	0.166	4	0.207	0.030	0.0009	0.146
Clay -15 m	AC251	10	0.295	0.063	0.0040	0.215					
Clay -6 m	AC075	9	0.147	0.024	0.0006	0.160					
Clay -9,5 m	AC090	15	0.134	0.024	0.0006	0.177	5	0.110	0.037	0.0014	0.335
Sandy silty clay (Echteld)	AC251	7	0.314	0.115	0.0133	0.366					
Sandy silty clay (Wijchen)	AC075	13	0.187	0.027	0.0007	0.146					
Sandy silty clay (Wijchen)	AC251	6	0.525	0.349	0.1218	0.664					
Humic clay	AC075	17	0.171	0.081	0.0066	0.475	9	0.184	0.084	0.0071	0.459
Humic clay	AC090	17	0.133	0.031	0.0010	0.237	7	0.127	0.041	0.0017	0.323
Humic clay	AC251	23	0.181	0.031	0.0010	0.170	7	0.183	0.025	0.0006	0.134
Eutrophic peat	AC090	21	0.159	0.056	0.0031	0.351	7	0.156	0.022	0.0005	0.138
Eutrophic peat	AC251	7	0.194	0.024	0.0006	0.124	6	0.226	0.069	0.0048	0.306
Mesotrophic peat	AC075	20	0.169	0.027	0.0007	0.161	5	0.184	0.041	0.0017	0.222
Mesotrophic peat	AC090	15	0.153	0.020	0.0004	0.129	6	0.149	0.018	0.0003	0.121
Mesotrophic peat	AC251	19	0.171	0.029	0.0009	0.172	7	0.235	0.105	0.0110	0.446
Peat deep	AC075	15	0.267	0.079	0.0063	0.297	5	0.304	0.094	0.0088	0.309
Peat deep	AC090	15	0.244	0.108	0.0117	0.443	5	0.181	0.074	0.0055	0.410
Peat deep	AC251	16	0.313	0.057	0.0032	0.181	5	0.310	0.038	0.0015	0.124
Peat compact / Basal peat	AC075	13	0.254	0.090	0.0081	0.355					
Peat compact / Basal peat	AC090	8	0.297	0.078	0.0061	0.262					
Peat compact / Basal peat	AC251	14	0.538	0.299	0.0893	0.556	4	0.351	0.092	0.0084	0.262

Table 5.1 Statistics of the cone penetration resistance per soil layer for class 1 cone and class 1+ cone

Table 5.1 gives an overview of the statistics of the cone penetration resistance data. It is interesting to note that for the various soil types the coefficient of variation (CoV) of the cone penetration resistance varies per location. So the variability of the cone penetration resistance of a certain soil type is not constant. This may imply that the conditions in a depositional environment also vary for different locations. Note that the reported CoV's are the result of various uncertainties: geological variability, measurement accuracy, uncertainties in soil unit weight and pore water pressure and errors in the interpretation of the CPT data. The contribution of each of these individual uncertainties to the reported CoV's is not investigated.
Furthermore the coefficient of variation of some of the soil layers is larger for the class 1 cones compared to the class 1+ cone. The class 1 cone has the advantage of the information of the sleeve friction and pore water pressure which is very helpful for the interpretation of the CPT data. The measurement accuracy of the cone penetration resistance of the class 1+ cone is however about four times higher than the class 1 cone. So both effects will play a role

in the resulting coefficient of variation. The more accurate 1+ cone not necessarily gives a lower uncertainty in q_{net} estimate.
The coefficient of variation of the corrected cone penetration resistance q_{net} and normalised cone penetration resistance Q_t is much larger than the coefficient of variation of the measured cone penetration resistance q_c. This can be attributed to the applied corrections and normalization as described in Paragraph 5.2. The coefficient of variation of the measured cone penetration resistance q_c and normalised cone penetration resistance Q_t are not in Table 5.1.

5.4 Correlation length

The horizontal correlation lengths of the measured cone penetration resistance q_c and the normalized cone penetration resistance Q_t for the various soil layers at the three locations are calculated with the semivariogram using equation 3.5 and correlation function using equations 3.2, 3.3 and 3.4. Note that the horizontal correlation length is calculated based on the mean values of the cone penetration resistances per soil layer and per CPT. So, the vertical variability within a soil layer in each CPT is thought to be averaged on the scale of a slip surface, as the vertical correlation length is assumed to be very short according to TAW (2002).

Semivariogram

Figure 5.21 and Figure 5.22 show the semivariogram of the measured cone penetration resistance q_c and the normalized cone penetration resistance Q_t of various clays.

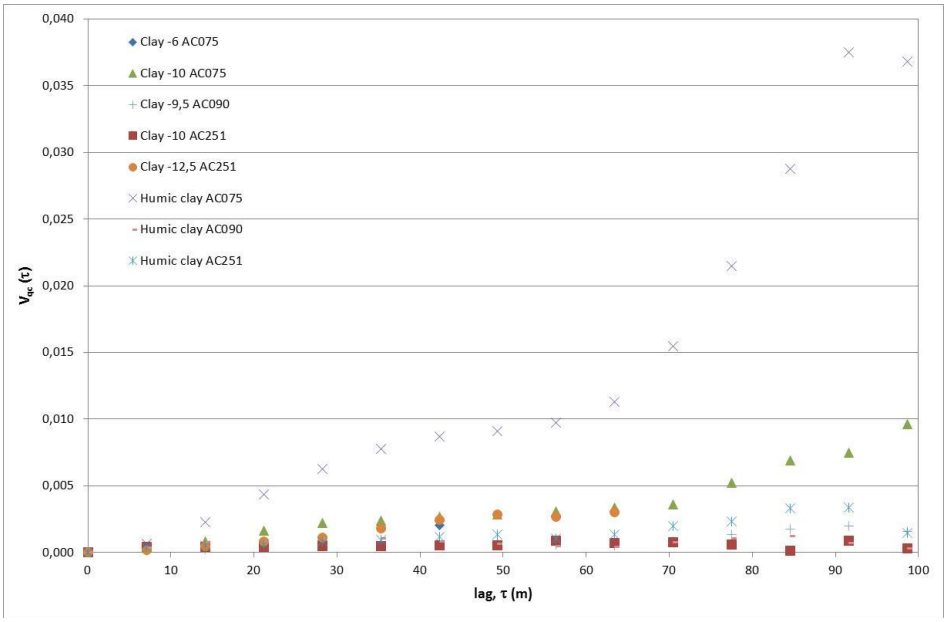

Figure 5.21 Semivariogram of the measured cone penetration resistance q_c of various clays

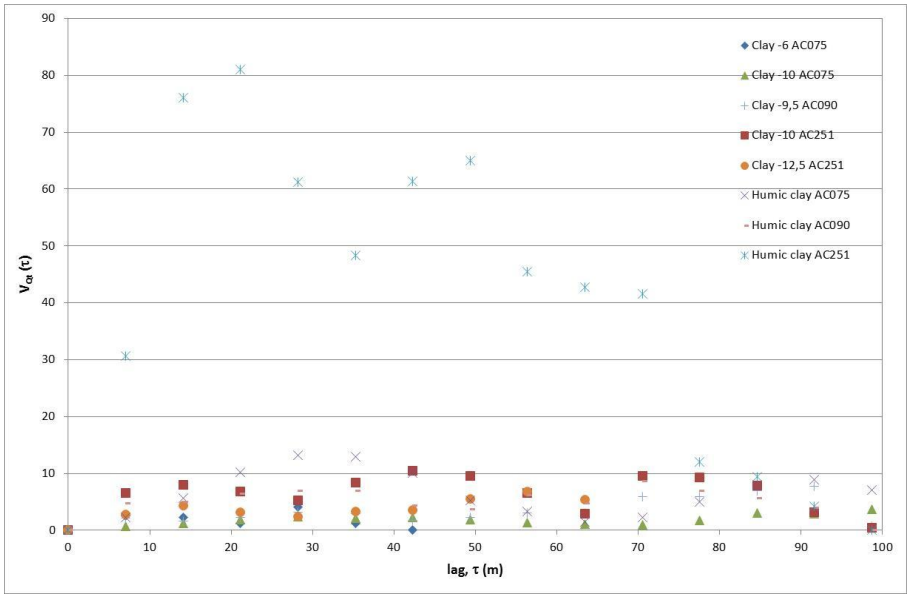

Figure 5.22 Semivariogram of the normalized cone penetration resistance Q_t of various clays

Using the semivariogram no clear results could be found. Figure 5.21 and Figure 5.22 show the semivariogram of various clay layers at the three measurement locations. Figure 5.21 shows the semivariogram when applying the semivariogram to the measured cone resistance q_c. Figure 5.22 shows the semivariogram when applying the semivariogram to the normalized cone resistance Q_t. Both figures show poor results, however it seems that the correlation length is larger for the measured cone resistance q_c compared to the normalized cone resistance Q_t.

Correlation function

Figure 5.23, Figure 5.24 and Figure 5.25 show the correlation function of the measured cone penetration resistance q_c and the normalized cone penetration resistance Q_t of various clays and peat.

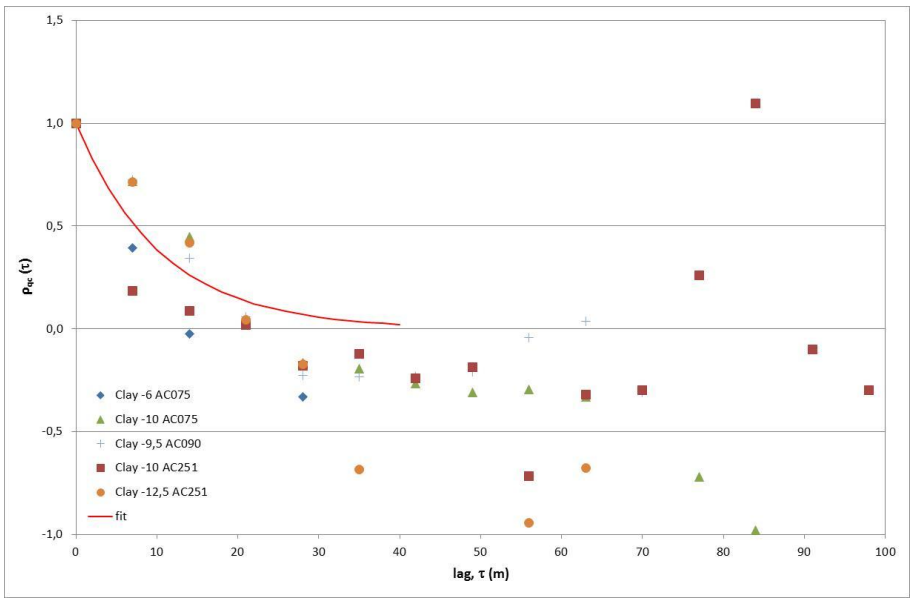

Figure 5.23 Correlation function of the measured cone penetration resistance q_c of various clays

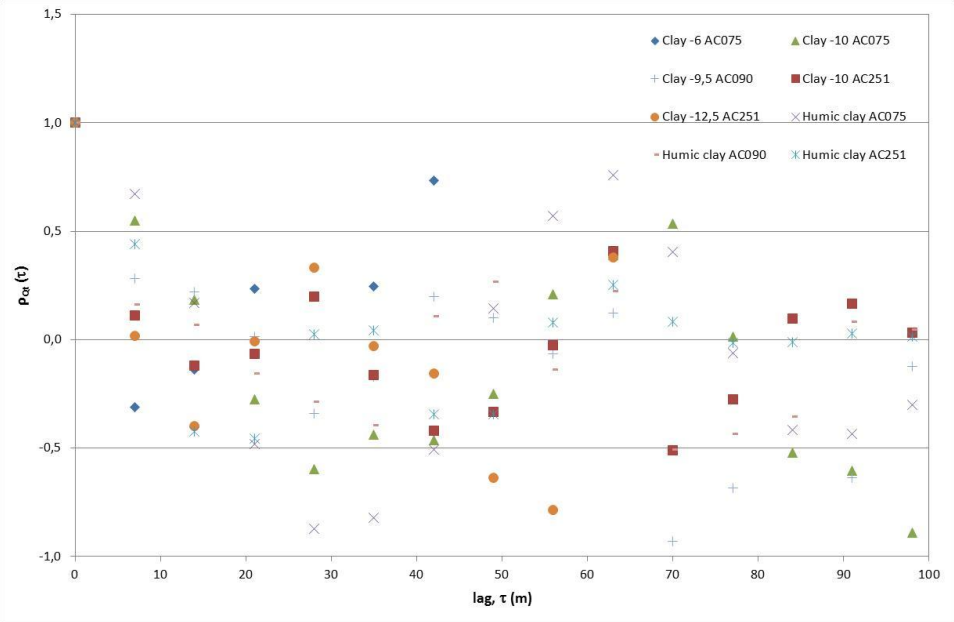

Figure 5.24 Correlation function of the normalized cone penetration resistance Q_t of various clays

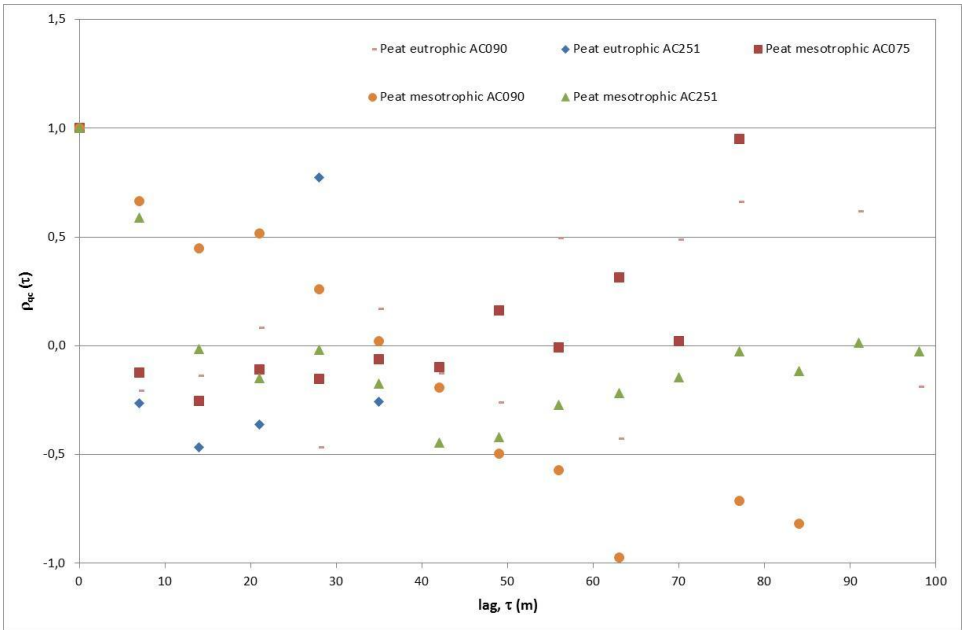

Figure 5.25 Correlation function of the measured cone penetration resistance q_c of various peat

From Figure 5.23 and Figure 5.25 it can be seen that the correlation function gives more distinct results for the correlation length compared to the semivariogram. In these figures the correlation function is applied to the measured cone resistance q_c. Only in Figure 5.23, a consistent result is obtained and a correlation function is plotted here. The correlation length seems to be not a constant for a depositional environment. From the derived results it can be seen that the correlation length differs for soil layers of the same soil type at different locations. The calculated horizontal correlation lengths for clay based on q_c (Figure 5.23) are generally much larger than the calculated correlation lengths for peat (Figure 5.25). It seems to be likely that the very different genesis of these soils is the cause of these different

correlation lengths. Sometimes the correlation of q_c shows a trend, for example clay at -12.5 m at location AC 251 (orange dots) in Figure 5.23. These trends disappear when calculating the correlation based on the normalized cone penetration resistance Q_t. So the normalization for effective stress level is important to remove trends in the data.
When applying the correlation function to the normalized cone penetration resistance Q_t, as presented in Figure 5.24, the derived correlation length is also unclear, similar to the semivariogram. For Q_t the correlation length is much shorter than for q_c. This seems to be in agreement with the results from the semivariogram. The poor results when applying the correlation function to Q_t can be caused by the corrections for measured pore water pressure and total vertical stress and normalisation with vertical effective stress as discussed in Paragraph 5.2 and Paragraph 5.3. Due to the uncertainties in this corrections and normalisation additional uncertainty is introduced in Q_t.
As discussed in Paragraph 3.2 it can be seen in Figure 5.23 and Figure 5.25 that the determination of the correlation length becomes unreliable after a certain distance. In these figures much scatter is found at distances larger than 30 m. The correlation often dips below zero and sometimes also below 1.0, which is theoretically not possible. The low correlation can be caused by the uncertainty in the estimation of the average values of q_c and Q_t as pointed out in Paragraph 3.2.1. Hence, especially correlations at larger lag distance should not be considered for further analysis. When working with Q_t additional noise can be introduced because of the various uncertainties as mentioned before. Due to these uncertainties the calculated correlation lengths of Q_t are less reliable. The calculated correlation lengths of q_c are probably more reliable, because there are less uncertainties, however in these correlation lengths the correction for trends is lacking.

Table 5.2 gives an overview of the horizontal correlation lengths θ of the measured cone penetration resistances q_c based on the class 1 cones and class 1+ cones as derived with the correlation function (see Paragraph 3.2).
The variance reduction factor Γ^2 is also given in the table. This variance reduction factor is calculated according to Vanmarcke (1977) using equation 3.6. So this variance reduction factor is related to the horizontal correlation length and the length of a potential slip surface, which is assumed here as 75 m. As proposed by Vanmarcke the variance reduction factor decreases when the dimension of a slip surface in horizontal direction increases.
The horizontal correlation lengths are calculated based on the mean values of the cone penetration resistances per soil layer and per CPT as mentioned before. The vertical variability within a soil layer in each CPT is thought to be averaged on the scale of a slip surface, because the vertical correlation length is assumed to be very short. Therefore the calculated variance reduction factor Γ^2 according to Vanmarcke accounts for the averaging of the horizontal fluctuation of the cone penetration resistance on the scale of a slip surface. Note that this definition of the variance reduction factor differs from the definition used in TAW (2002) and Calle (2007) as discussed in Paragraph 3.1.

Soil type	Location	$\theta_{qc,class\ 1+}$ (m)	$\theta_{qc,class1}$ (m)	Γ^2 ($\theta_{qc,class\ 1+}$) (-)	Γ^2 ($\theta_{qc,class\ 1}$) (-)
Clay -10 m	AC075	21	30	0.28	0.40
Clay -10 m	AC251	9	30	0.12	0.40
Clay -11 m	AC075				
Clay -12,5 m	AC251	21		0.28	
Clay -15 m	AC251				
Clay -6 m	AC075	9		0.12	
Clay -9,5 m	AC090	21	15	0.28	0.20
Sandy silty clay (Echteld)	AC251				
Sandy silty clay (Wijchen)	AC075				
Sandy silty clay (Wijchen)	AC251				
Humic clay	AC075	21	28	0.28	0.37
Humic clay	AC090	14	10	0.19	0.13
Humic clay	AC251	21	30	0.28	0.40
Eutrophic peat	AC090	3	10	0.04	0.13
Eutrophic peat	AC251	3		0.04	
Mesotrophic peat	AC075	3	10	0.04	0.13
Mesotrophic peat	AC090	33	20	0.44	0.27
Mesotrophic peat	AC251	12	30	0.16	0.40
Peat deep	AC075	15	30	0.20	0.40
Peat deep	AC090	3	30	0.04	0.40
Peat deep	AC251	30	30	0.40	0.40
Peat compact / Basal peat	AC075				
Peat compact / Basal peat	AC090				
Peat compact / Basal peat	AC251	5		0.07	

Table 5.2 Derived horizontal correlation lengths of the measured cone penetration resistance q_c based on the class 1 cones and class 1+ cones. The related variance reduction factor is also given.

Table 5.2 shows a large variation in correlation lengths for the various soil types. The length over which the correlation dies out varies with a factor two to ten. Consequently also the variance reduction factor has a large variation. These findings seem to correspond very well with the results in the previous paragraph where the coefficient of variation was also not constant for a certain soil type. As the calculated horizontal correlation length varies considerably it may be that the spatial variability of the cone penetration resistance is very different at the three locations. It is also possible that the various uncertainties as discussed before play an important role on the results.

Furthermore the reliability of the correlation length based on the CPT's with class 1 cone is less than the correlation length based on the CPT's with class 1+ cones because of the limited number of CPT's with class 1 cone and the fact that the calculated correlation length is in the same order as the distance between the CPT's with class 1 cone.

Overall the horizontal correlation length ranges between 3 and 33 m resulting in a variance reduction factor between 0.04 and 0.44. The average value of the variance reduction factor is 0.19. The calculated horizontal correlation lengths are relatively short compared to the horizontal correlation length of 50 to 100 m as mentioned in TAW (2002). The calculated correlation lengths are also relatively short compared to the assumed dimensions of a slope

failure of 75 m. As a consequence the calculated variance reduction for the horizontal direction is relevant, at least for the shortest correlation lengths. Although the approach of TAW (2002) and Calle (2007) differs from the approach of Vanmarcke (1977) the range of the calculated variance reduction factors compare very well with the recommended variance reduction factor Γ^2 is 0.25 in TAW (2002).
When working with the normalized cone penetration resistance Q_t the calculated horizontal correlation length is shorter (3 - 13 m) and consequently the variance reduction factor becomes smaller (0.04 - 0.17).
As each series of CPT's concern the scale of a slip surface of a potential slope failure the CPT data is deemed to be a local data set, for which TAW (2002) recommends a variance reduction factor Γ^2 is 0. So the calculated variance reduction factor based on the measured cone penetration resistances q_c is relatively high compared with the variance reduction factor in TAW (2002).

5.5 Local data versus regional data

The local CPT data from the three research locations with class 1+ cones is compared with the regional data set based on 72 CPT's with class 1 cones from Waterboard Rivierenland (WSRL) (see also Paragraph 4.2). The class 1 CPT's from Waterboard Rivierenland are located along a stretch of about 12.5 km along the drainage canal Achterwaterschap. The three research locations with class 1+ cones are situated within this stretch. Note that the CPT's from Waterboard Rivierenland are performed in the crest of the dike, whereas the class 1+ CPT's are performed at the toe. In the crest of the dike a higher vertical effective stress may be expected. Consequently the cone penetration resistance in the crest of the dike may be (on average) somewhat higher.

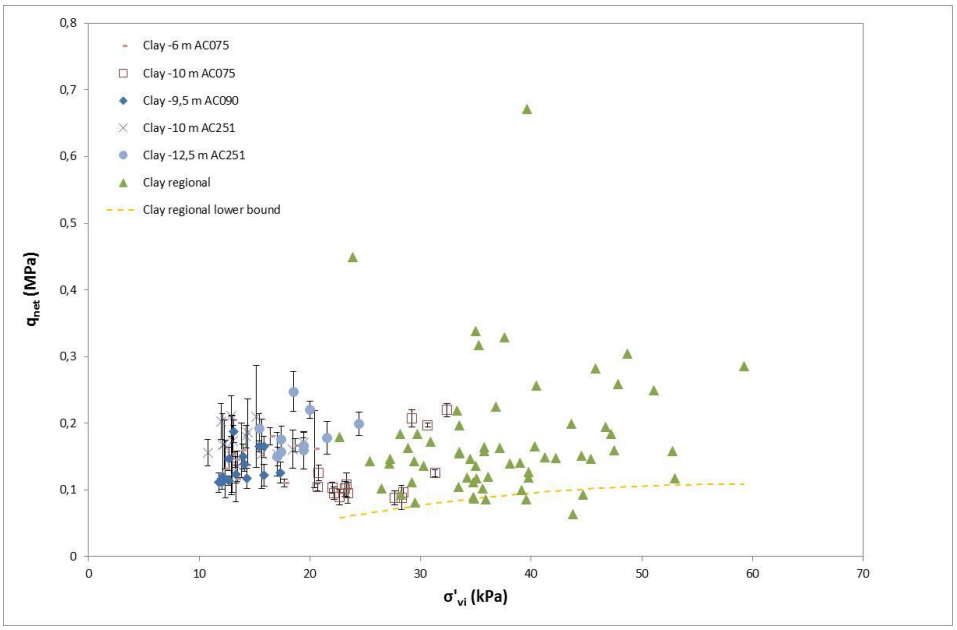

Figure 5.26 Comparison between local CPT data at three locations and regional CPT data from Waterboard Rivierenland for clay

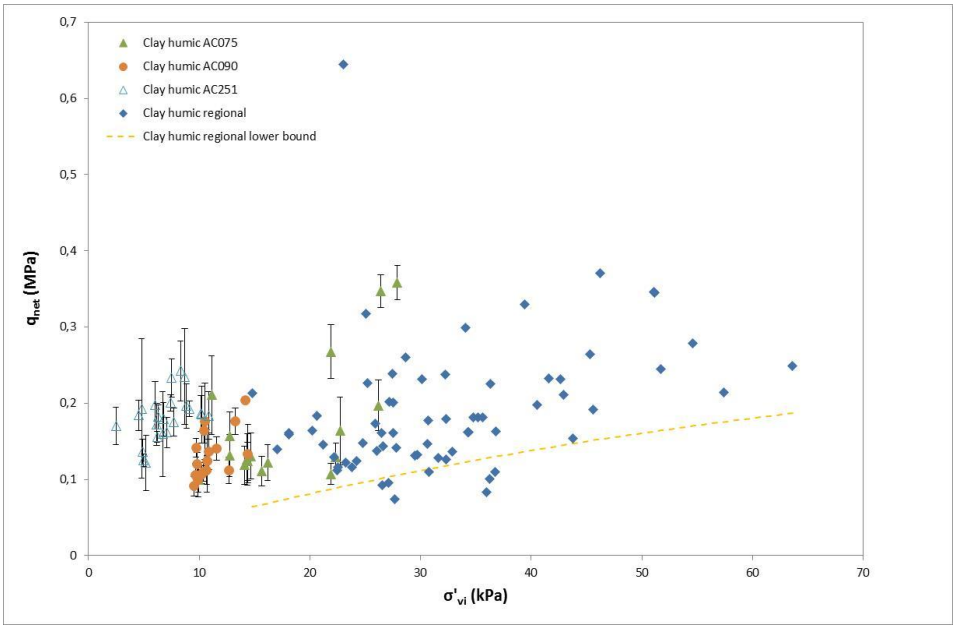

Figure 5.27 Comparison between local CPT data at three locations and regional CPT data from Waterboard Rivierenland for humic clay

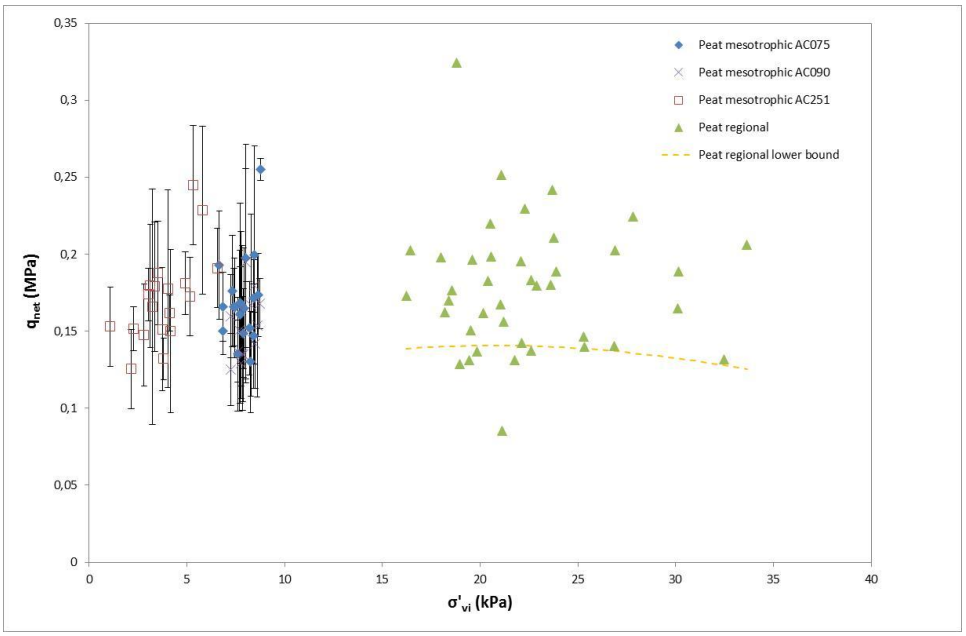

Figure 5.28 Comparison between local CPT data at three locations and regional CPT data from Waterboard Rivierenland for mesotrophic peat

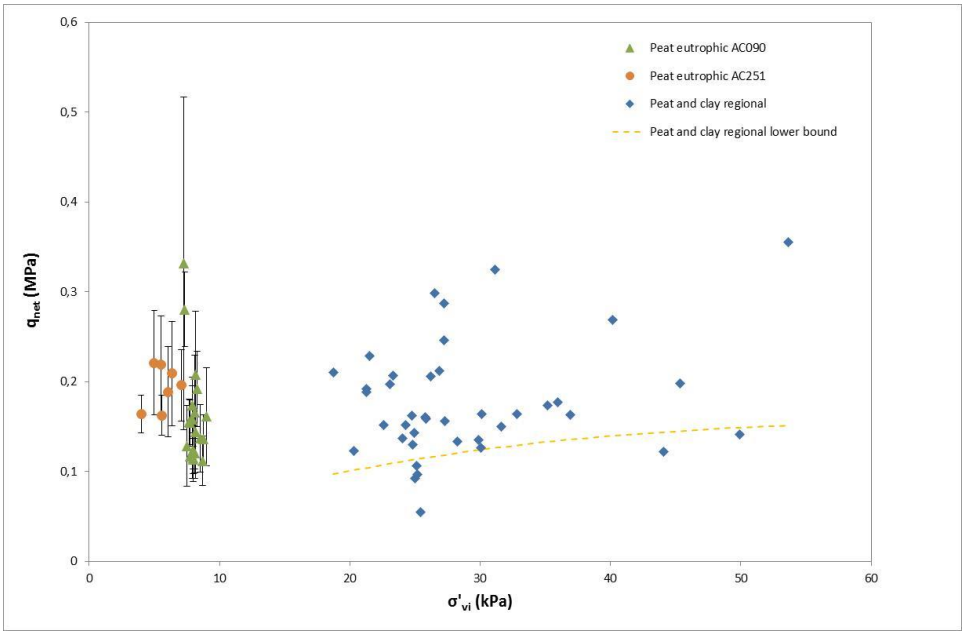

Figure 5.29 Comparison between local CPT data at three locations and regional CPT data from Waterboard Rivierenland for eutrophic peat

Figure 5.26, Figure 5.27, Figure 5.28 and Figure 5.29 show the results of the comparison between the local CPT data from the three research locations with the regional CPT data. The corrected cone penetration resistance q_{net} is plotted against effective vertical stress. Each symbol of the local CPT data represents the mean value of the corrected cone resistance of the concerning soil layer within one CPT. At each symbol the 90% confidence interval is given.
In the figures it is clear that the effective vertical stress at the toe of the dike is somewhat lower than the effective vertical stress below the crest of the dike. The variation of the effective stress in the crest of the dike is large, compared to the toe of the dike. It seems that the cone penetration resistance of the local CPT data is in the same order of magnitude as the regional CPT data. So, the low stress level at the toe of the dike has a limited effect on the cone penetration resistance compared to the regional CPT data. This is understandable because the stress dependency in the regional data set is not very large too, excepted for humic clay (see Figure 5.27).
The degree of variability within the soil layers at the three research locations based on the mean values per CPT relative to the variability of the regional dataset is large. Visual the local variability of the mean values is roughly about half the regional variability. Sometimes the local variability is larger than 50% of the regional variability. This is the case for humic clay at location AC 075 (Figure 5.27), mesotrophic peat at AC 075 and AC 251 (Figure 5.28) and eutrophic peat at location AC 090 (Figure 5.29). As can be seen from the plotted 90% confidence intervals of the peat layers the variation of the cone penetration resistance within one CPT can also be very large compared to the regional CPT data.

Variance ratio and variance reduction factor
In Table 5.3 the numbers of the comparison between the local CPT data at three locations and regional CPT data from Waterboard Rivierenland (WSRL) are presented. The ratio α of the local variance σ_{loc}^2 and the regional variance σ_{reg}^2 of the cone penetration resistances is calculated according to Calle (2007 and 2008), as described in Paragraph 3.1. From this ratio also the variance reduction factor Γ^2 can be calculated. Here the local variance σ_{loc}^2 is calculated per location and per soil layer from the means of the cone penetration resistances

of the CPT's which are available per soil layer at the concerning location (see Table 5.3). The regional variance σ_{reg}^2 is based on the data from the mean cone penetration resistances per soil layer form 72 CPT's from Waterboard Rivierenland (standard deviations are reported in Paragraph 4.2, Table 4.2). The local data of the three locations is not integrated in the regional data from Waterboard Rivierenland, because of the different measurement accuracy of the cones (class 1 versus class 1+) and the different locations of the CPT's (crest versus toe) as mentioned before. The outcome of this analysis gives unexpected results. The values of the ratio α are relative low. Consequently the values of Γ^2 are relatively high. This becomes clear when these values are compared with the Γ^2 values derived from the correlation length θ as described in Paragraph 5.4.
To verify these results of α and Γ^2 the CPT data of the three research locations is combined to calculate an alternative regional dataset. This alternative regional dataset is called "merged local data" in Table 5.3. The mean values, standard deviations and variances are mentioned in Table 5.3 per soil type. With this alternative regional dataset the ratio α of the local variance σ_{loc}^2 and the regional variance σ_{reg}^2 is calculated using the combination of the local CPT data as a regional dataset. As can be seen from Table 5.3 the results from this analysis are comparable with the results obtained using the regional variance σ_{reg}^2 based on the regional CPT data from Waterboard Rivierenland. These results are not comparable with the default value for regional data according to TAW (2002) with an α of 0.75 (Γ^2 = 0.25). Until now these results are not understood. Perhaps the unaccountable results can be explained by the differences between the datasets as mentioned before: CPT's with class 1 cone versus CPT's with class 1+ cone and CPT's located in the crest versus CPT's located at the toe.

Soil type	Loca-tion	Local data three locations				α_{qnet} (σ^2_{loc}/ $\sigma^2_{reg,WSRL}$) regional data from WSRL	α_{qnet} (σ^2_{loc}/ $\sigma^2_{reg,merge}$) regional data is merged local data	Γ^2 (α_{qnet}) regional data from WSRL	Γ^2 (α_{qnet}) regional data is merged local data
		n	$\mu\ q_{net}$	$\sigma\ q_{net}$	$\sigma^2\ q_{net}$				
Clay -10 m	AC075	15	0,123	0,046	0,002	0,21	0,51	0,79	0,49
Clay -10 m	AC251	15	0,172	0,022	0,001	0,05	0,12	0,95	0,88
Clay -11 m	AC075	8	0,152	0,054	0,003	0,29	0,71	0,71	0,29
Clay -12,5 m	AC251	10	0,185	0,031	0,001	0,09	0,23	0,91	0,77
Clay -15 m	AC251	10	0,295	0,063	0,004	0,40	0,98	0,60	0,02
Clay -6 m	AC075	9	0,147	0,024	0,001	0,06	0,13	0,94	0,87
Clay -9,5 m	AC090	15	0,134	0,024	0,001	0,06	0,14	0,94	0,86
Clay merged	all	82	0,168	0,064	0,004				
Sandy silty clay (Echteld)	AC251	7	0,314	0,115	0,013				
Sandy silty clay (Wijchen)	AC075	13	0,187	0,027	0,001				
Sandy silty clay (Wijchen)	AC251	6	0,525	0,349	0,122				
Humic clay	AC075	17	0,171	0,081	0,007	0,81	2,34	0,19	
Humic clay	AC090	17	0,133	0,031	0,001	0,12	0,35	0,88	0,65
Humic clay	AC251	23	0,181	0,031	0,001	0,12	0,34	0,88	0,66
Humic clay merged	all	60	0,163	0,053	0,003				
Eutrophic peat	AC090	21	0,159	0,056	0,003	0,87	1,16	0,13	
Eutrophic peat	AC251	7	0,194	0,024	0,001	0,16	0,22	0,84	0,78
Eutrophic peat merged	all	28	0,168	0,052	0,003				
Mesotrophic peat	AC075	20	0,169	0,027	0,001	0,46	0,57	0,54	0,43
Mesotrophic peat	AC090	15	0,153	0,020	0,000	0,24	0,30	0,76	0,70
Mesotrophic peat	AC251	19	0,171	0,029	0,001	0,54	0,67	0,46	0,33
Mesotrophic peat merged	all	53	0,171	0,036	0,001				
Peat deep	AC075	15	0,267	0,079	0,006	3,94	0,84		0,16
Peat deep	AC090	15	0,244	0,108	0,012	7,33	1,56		
Peat deep	AC251	16	0,313	0,057	0,003	2,01	0,43		0,57
Peat deep merged	all	46	0,276	0,087	0,008				
Peat compact / Basal peat	AC075	13	0,254	0,090	0,008		0,14		0,86
Peat compact / Basal peat	AC090	8	0,297	0,078	0,006		0,11		0,89
Peat compact / Basal peat	AC251	14	0,538	0,299	0,089		1,59		
Peat compact / Basal peat merged	all	35	0,378	0,237	0,056				

Table 5.3 Statistics of the cone penetration resistances per soil layer for CPT's with class 1+ cone and calculated ratio's of local and regional variance and related variance reduction factor

5.6 Summary

The analysis of the CPT data at three locations along the Achterwaterschap show a large variability in the stratigraphy. There is also a large variability in the cone penetration resistance. This is the case for the variability in vertical direction within the CPT's as well as for the variability in horizontal direction as derived from the means of the cone penetration resistances of the CPT's within a soil layer. Continuous very soft layers are not identified at the three locations along the Achterwaterschap. Many 'outliers' are identified in the cone penetration resistances. These outliers are attributed to fragments of wood in the peat and humic clay layers.

The corrections and normalisation of the CPT data have an important effect on the cone penetration resistances. The coefficient of variation of the corrected cone penetration resistance q_{net} and normalised cone penetration resistance Q_t is much larger than the coefficient of variation of the measured cone penetration resistance q_c. The corrections and normalization will affect the results of the analyses. However the coefficient of variability of the class 1 cone and the class 1+ cone are comparable. So the effect of the uncertainty about stratigraphy when interpreting the class 1+ data seems to be as large as the effect of the differences in measurement accuracy between the class 1 cone and the class 1+ cone. However, the uncertainty about the variability in soil unit weight and pore water pressure within the soil layers affect the analysis of CPT data from both class 1 cone and class 1+ cone.

Correlation lengths between 3 and 33 m are found based on the measured cone penetration resistances q_c from the class 1+ CPT's using the correlation function. The correlation length varies for different soil types but also for the same soil type the correlation length is variable. This is the same with the coefficient of variation of the cone penetration resistance. So the variability within a certain depositional environment is likely to be variable enough to result in very different degrees of variability from one location to another. For peat layers the correlation length is generally shorter than for clay layers. This can be expected based on the very different genesis of these soils.

Calculating the variance reduction factor Γ^2 based on the horizontal correlation length (3 - 33 m) as determined for the measured cone penetration resistance q_c results in values between 0.04 and 0.44, with an average value of 0.19. As the horizontal correlation length is calculated based on the mean values of the cone penetration resistances per soil layer and per CPT this variance reduction factor Γ^2 accounts for the local averaging of the horizontal fluctuation of the cone penetration resistance on the scale of a slip surface. Although the approach of TAW (2002) and Calle (2007) differs from the approach of Vanmarcke (1977) the range of the calculated variance reduction factors compare very well with the recommended variance reduction factor Γ^2 of 0.25 in TAW (2002). Considering that the CPT data at the three locations are local data on the scale of a potential slope failure these results are higher than the variance reduction factor of 0 in TAW (2002).

Using the normalised cone penetration resistance Q_t the calculated horizontal correlation lengths are relatively short (3 - 13 m). Consequently the variance reduction factor (0.04 - 0.17) is lower than the variance reduction factor based on the measured cone penetration resistance q_c. These results may be influenced by the interpretation, corrections and normalisation as mentioned before. On the other hand the normalised cone penetration resistance Q_t is theoretically a more decent parameter to calculate the correlation length and coefficient of variation, because of the corrections and the normalization which removes trends.

Using the ratio α of the local variance σ_{loc}^2 and the regional variance σ_{reg}^2 to determine the variance reduction factor Γ^2 gives results (0.13 – 0.95) which are not understood until now. These results are generally very high compared to the suggested variance reduction factor of 0.25 for regional data in TAW (2002). The results in this study are in agreement with TAW

(2002) as far as the results found in this study show that the variance reduction factor for regional data is generally higher than the variance reduction factor for local data.
The local variability of the cone penetration resistance at the three locations is significant compared to the regional variability. This is especially the case for humic clay, mesotrophic peat and eutrophic peat. For these soil layers the local variability is more than 50% of the regional variability.

6 Conclusions

The variability of the subsoil at three locations along the Achterwaterschap is found to be considerable. Successive cone penetration tests with an interval of 7 meters over a stretch of 100 m show a continuous variation in soil stratigraphy and cone penetration resistance. In accordance with common geotechnical practice in infrastructural projects, safety assessments and design of flood defences where CPT's are carried out with intervals of 100 m or more, it has to be concluded that one CPT is only a random sample of the stratigraphy and cone penetration resistance. The significance of one CPT to describe the stratigraphy and cone penetration resistance for a stretch of 100 m or more is very low. A second CPT close to the first one or at somewhat larger distance can give a very different result. The stratigraphy may be different and the cone penetration resistance can be substantially higher or lower. Related to the failure mechanism of slope instability where the size of a potential slip surface is in the order of 50 to 100 m, one CPT is not enough to determine a reliable mean and standard deviation of the shear strength on the slip surface.

The present approach is to estimate the local shear strength of the soil based on only one local CPT, with the characteristic lower bound value about 35% lower than the men value, mainly due to transformation uncertainty (Deltares, 2014). At the three Achterwaterschap locations it is observed that the variation in cone penetration resistance within the series of CPT's is larger than 35%. This means that when a relatively high cone penetration resistance occurs in one CPT the characteristic lower bound can be higher than the mean value based on a larger number of CPT's. When a relatively low cone penetration resistance occurs the characteristic lower bound can be much lower than the characteristic lower bound based on a larger number of CPT's. So the determination of the shear strength based on one CPT is not reliable.

Interpretation of the CPT's also determines the variation of the derived stratigraphy and coefficient of variation of the cone penetration resistance. When interpreting CPT's there are always difficulties because the information from CPT's is limited. Insufficient information on soil unit weight and pore water pressure for example can have a large influence on the results of the interpretation. These limitations cause noise in the results of the CPT interpretation. The coefficient of variation of the corrected cone penetration resistance q_{net} and normalised cone penetration resistance Q_t are much larger than the coefficient of variation of the measured cone penetration resistance q_c. Another issue is the measurement inaccuracy. This measurement accuracy also determines the coefficient of variation of the cone penetration resistance. The contribution of each of these uncertainties to the total uncertainty is not quantified in this study.

Based on these observations it can be concluded that the characteristic lower bound of the cone penetration resistance for a dike section has to be derived from a series of CPT's. This series of CPT's represent the variability of the soil much more than one CPT. These series of CPT's can belong to a dike section or a WBI-SOS segment for example. Averaging of variability along a slip surface can be taken into account by the variance reduction factor as mentioned in TAW (2002). This research generally confirms the suggested values in TAW (2002) as far as the results found in this study show that the variance reduction factor for regional data is generally higher than the variance reduction factor for local data. This variance reduction factor seems to be also very variable with dense datasets; the variance reduction factor is not a specific value for a deposit or soil type. The characteristic lower bound can be calculated using a log normal distribution.

Individual low cone penetration resistances can be identified in a site investigation, however considering the random pattern of the variability as identified in this project these low resistances will not have a large effect on the mobilized shear strength along a potential slip

surface because the variability of the shear strength averages along the slip surface. Continuous very soft layers are not identified at the three locations along the Achterwaterschap.

7 Recommendations

General recommendations

Based on the observations at the three locations at the "Achterwaterschap" it is recommended to calculate the characteristic lower bound of the shear strength from a series of CPT's. This series of CPT's represent the variability of the soil much more than one CPT.

When taking the common practice of distances between CPT's as starting point it is recommended to derive the characteristic lower bound of the shear strength from a series of CPT's. These series of CPT's can belong to a dike section or a WBI-SOS segment for example. At least 5 to 10 CPT's have to be combined for the calculation of the characteristic lower bound of the shear strength.

For the assessment of slope stability the extreme values of the shear strength on a potential slip surface are not important but the average strength is important. Therefore the uncertainty of the shear strength can be reduced by accounting for averaging of the uncertainty. The variance reduction factor Γ^2 = 0.25 from TAW (2002) is recommended as this research generally confirms the suggested values in TAW (2002) as far as the results found in this study show that the variance reduction factor for regional data is generally higher than the variance reduction factor for local data (Γ^2 = 0 according to TAW (2002).

For the statistical analysis to calculate the characteristic lower bound value the corrected cone resistance q_{net} or the normalised cone resistance Q_t can be used. The cone resistance Q_t is normalised for the vertical effective stress. Using the normalised cone resistance Q_t makes it possible to apply straightforward statistical analysis. When using the corrected cone resistance q_{net} the least squares method can be applied to derive the characteristic lower bound values of the relationship between effective stress and corrected cone resistance.

Local optimization

In some cases it is desired to optimize the shear strength of a dike section. Carrying out a series of CPT's can be helpful. The number of CPT's and the distance between the CPT's has to cover the scale of a potential slip surface. This local set of CPT's can be used to calculate a local value of the characteristic lower bound of the shear strength. For this local characteristic value it is allowed to apply the variance reduction factor Γ^2 = 0 according to TAW (2002).

Optimization of variance reduction factor

In special situations it may be helpful to optimize the variance reduction factor Γ^2 for regional sets of CPT data. Optimization of the variance reduction factor may result in a smaller distance between the mean value of the shear strength and the characteristic lower bound. As illustrated in this study the analyses and the interpretation of the results of the analyses are not straightforward. To optimize the variance reduction factor it is recommended to:

- Perform some series of CPT's at different locations in a project. One series of CPT's has to consist of 5 to 10 CPT's and the distance between the CPT's has to be in the order of 5 m.
- Before performing the Series of CPT's carry out the regular CPT's for the site investigation. Based on the regular CPT's the locations for the series of CPT's can be chosen. To choose the locations of the series of CPT's it is recommended to use as much as possible geological data: WBI-SOS, DINO, geological maps.

- For the interpretation of the CPT's it is helpful when information of the soil unit weight and pore water pressure is available. This information improves the reliability of the CPT interpretation.
- Based on the regular CPT's the regional variance of the cone penetration resistance can be calculated. The local variance of the cone penetration resistance can be calculated from the series of CPT's. From the series of CPT's also the correlation length can be calculated.
- It is recommended to apply various statistical methods to calculate the correlation length. Preferably the correlation length will be not only determined with the common correlation function, but also with more complex approaches such as Bayesian approach or Maximum Likelihood. These more complex approaches may give more distinct results.
- Based on the ratio of the local variance of the cone penetration resistance and regional variance of the cone penetration resistance the variance reduction factor can be calculated. Calculation of the variance reduction factor is also possible from the correlation length. It can be assumed that the variance reduction factor is the same for s_u, S, m, POP/OCR. It seems to be likely that spatial variability of these parameters result from variability of the basic soil properties, such as clay content and organic content.
- With the results of the previous steps the characteristic lower bound of the shear strength can be calculated. Again the corrected cone resistance q_{net} or the normalised cone resistance Q_t can be applied. In this step averaging of the uncertainty is applied based on the optimized variance reduction factor Γ^2.

Further research

As this research demonstrates the various uncertainties in processing the CPT data, it is recommended to perform additional research with field and laboratory tests to obtain additional information regarding the variability of soil layers. This research can include bore holes with determination of soil unit weight and organic content and plasticity index or field vane tests. Soil unit weight can be used to improve the analyses of the CPT data in this research. Organic content and plasticity index can be used to determine the variance ratio and correlation length based on these parameters. The advantage of the latter parameters is that they are simple parameters without complex interpretation and they are not susceptible for sample disturbance. However, they give no information about the variability of the state (overconsolidation ratio) of the soil. Field vane tests can also be used to calculate the variance ratio and correlation length. Field vane tests give a direct measure of the undrained shear strength without effects of sample disturbance. As they measure the in situ strength the measurements include the variability of the state of the soil.

8 Consequenties voor WBI instrumentarium

Leidt het onderzoek tot aanpassing van de instrumenten voor toetsen van waterkeringen (zowel technisch als procedureel)?
→ Ja, invulling van leemte

Zo ja, welke aanpassingen dienen te worden doorgevoerd en hoe zijn deze te implementeren?
→ Schematiseringshandleiding macrostabiliteit aanpassen, CPT-tool aanpassen en Consistentie-tool uitbreiden; eventueel ook consequenties voor kalibratie veiligheidsfactoren. De aanpassing betreft dat voor het beoordelen van macrostabiliteit niet kan worden uitgegaan van de lokale schuifsterkte op basis van een enkele sondering, maar dat een regionale karakteristieke ondergrenswaarde moet worden toegepast op basis van een serie sonderingen. Deze serie sonderingen kan bijvoorbeeld behoren bij een of meerdere dijkvakken of een WBI SOS-segment. Voor lokale optimalisatie kan eventueel een serie sonderingen worden uitgevoerd op de schaal van een schuifvlak om op basis daarvan de lokale schuifsterkte te bepalen.
→ Samenhang met onderzoek over onzekerheid correlatiefactor N_{kt}
→ De verwachting is dat de aangepaste werkwijze leidt tot meer efficiëntie voor waterkeringbeheerders, omdat met regionale parameters wordt gewerkt en niet meer per dwarsprofiel andere parameters moeten worden afgeleid en toegepast.

Zo nee, waarom niet en wat is er eventueel nog voor nodig om wel tot een beter instrumentarium te komen?
→ n.v.t.

9 References

Been, K., and Jefferies, M.G. (1992). Towards systematic CPT interpretation. In Proceedings of the Wroth Symposium, Oxford, U.K. pp. 44–55.

Begemann, H.K. (1965). The Friction Jacket Cone as an Aide in Determining the Soil Profile. Proc. 6th. Int. Conf. on Soil Mechanics and Foundation Engineering. Montreal. Vol. 1, pp. 17-20.

Calle, E.O.F. (2007). Statistiek bij regionale proevenverzamelingen: Het ruimtelijk statistische model. Geotechniek, juli 2007.

Calle, E,O.F. (2008). Statistiek bij regionale proevenverzamelingen. Geotechniek, januari 2008.

Campanella, R.G. en Kokan, M.J. (1993). A new approach to measuring dilatancy in saturated sands. Geotechnical Testing Journal, ASTM, 16 (4), 485-95.

Cao, Z., Wang, Y., Li, D. (2017). Probabilistic Approaches for Geotechnical Site Characterization and Slope Stability Analysis. Springer-Verlag GmbH Berlin Heidelberg. ISBN 978-3-662-52912-6.

De Gast, T., Vardon, P.J., Hicks, M.A. (2017). Estimating Spatial Correlations under Man-Made Structures on Soft Soils. Geo-Risk 2017 GSP 284.

De Gast, T., Vardon, P.J., Hicks, M.A. (2018). Detection of soil variability using CPTs. In: Cone Penetration Testing 2018. Eds.: Hicks, M.A., Pisanò, F., Peuchen, J.

Deltares (2014). Dijken op Veen II, Eindrapport Heterogeniteit. Report 1208254-019-GEO-0001, Version 01, 30 april 2014, concept.

Fenton, G.A. (1999). Estimation for Stochastic Soil Models. Journal of Geotechnical and Geoenvironmental Engineering, Vol. 125, No. 6, June, 1999.

Gouw, M.J.P., Erkens, G. (2007) Architecture of the Holocene Rhine-Meuse delta (the Netherlands) – A result of changing external controls. Netherlands Journal of Geosciences — Geologie en Mijnbouw | 86 – 1 | 23 - 54 .

Hijma, M.P., Cohen, K.M., Hoffmann, G., Van der Spek, A.J.F., Stouthamer, E.. (2009) From river valley to estuary: the evolution of the Rhine mouth in the early to middle Holocene (western Netherlands, Rhine-Meuse delta). Netherlands Journal of Geosciences — Geologie en Mijnbouw | 88 – 1 | 13 - 53 .

I&M (2017). Schematiseringshandleiding macrostabiliteit. WBI 2017. Ministerie van Infrastructuur en Milieu. 15 november 2016.

Jefferies, M.G. and Davies, M.P. (1991). Soil classification by the cone penetration test: Discussion. Canadian Geotechnical Journal, 28, 1, 173–468.

Robertson, P.K. (1990). “Soil classification using the cone penetration test.” Can. Geotech. J., 27 (1), 151–158.

Robertson, P.K. (1999). “Estimation of minimum undrained shear strength for flow liquefaction using the CPT.” Proc., 2nd Int. Conf. On Earthquake Geotechnical Engineering, Balkema, Rotterdam, The Netherlands.

Spry, M. J., Kulhawy, F. H., Grigoriu, M. D. (1988). Reliability based foundation design for transmission line structures: Geotechnical site characterization strategy, Report EL-5507(1). Palo Alto, CA: Electric Power Research Institute.

TAW (2002). Technisch Rapport Waterkerende Grondconstructies. Technische Adviescommissie voor de Waterkeringen. Juni 2001. ISBN 90-369-3776-0.

Vanmarcke, E.H. (1977). Reliability of Earth Slopes. Journal of the Geotechnical Engineering Division. Vol. 103, No. GT11, November 1977.

Zhang, G., Robertson, P.K., and Brachman, R.W.I. (2002). “Estimating liquefaction induced ground settlements from CPT for level ground.” Can. Geotech. J., 39 (5), 1168–1180.